

UNCLASSIFIED

NASA Technical Memorandum 80136

DETERMINATION OF ASPS PERFORMANCE FOR LARGE PAYLOADS IN THE SHUTTLE ORBITER DISTURBANCE ENVIRONMENT

SLL 85-U-0752

CLAUDE R. KECKLER, KEMPER S. KIBLER, AND
LAWRENCE F. ROWELL

DISTRIBUTION STATEMENT A
Approved for public release; Distribution Unlimited

OCTOBER 1979

PLEASE RETURN TO:
BMD TECHNICAL INFORMATION CENTER
BALLISTIC MISSILE DEFENSE ORGANIZATION
7100 DEFENSE PENTAGON
WASHINGTON D.C. 20301-7100

NASA

National Aeronautics and
Space Administration

Langley Research Center
Hampton, Virginia 23665

UNCLASSIFIED

SEP 09 1985

19980513 284

u3918

Accession Number: 3919

Publication Date: Feb 26, 1973

Title: Characteristics of the Tropopause and Its Effect on Optical Imaging

Personal Author: Cotton, E.S.

Corporate Author Or Publisher: Lincoln Laboratory, Massachusetts Institute of Technology, Lexington, Report Number: TN 1973-15

Report Prepared for: Electronic Systems Division, Hanscom AFB, MA Report Number Assigned by Contract Monitor: SLL 80-174; ESD-TR-73-64

Comments on Document: Archive, RRI, DEW

Descriptors, Keywords: Characteristic Tropopause Optical Image Meteorology Path New Zealand Experiment Stratosphere Propagation

Pages: 00030

Cataloged Date: Nov 27, 1992

Contract Number: F19628-73-C-0002

Document Type: HC

Number of Copies In Library: 000001

Record ID: 25276

Source of Document: DEW

DETERMINATION OF ASPS PERFORMANCE FOR LARGE PAYLOADS
IN THE SHUTTLE ORBITER DISTURBANCE ENVIRONMENT

by

Claude R. Keckler, Kemper S. Kibler, and
Lawrence F. Rowell

SUMMARY

To accommodate projected requirements of large facility class payloads envisioned for the mid-1980's, payload auxiliary pointing systems have been proposed. The most promising of the various pointing system candidates is the Annular Suspension and Pointing System (ASPS) which utilizes magnetic suspension to achieve high accuracy pointing and stability, as well as isolation of the payload from carrier vehicle disturbances.

To determine the applicability of ASPS in satisfying mission objectives of large facility-class payloads, an analysis was conducted using a high fidelity simulation of ASPS, its payload, and the Shuttle orbiter. The objectives of this analysis were to define the worst case orientations of the ASPS and its payload for the various vehicle disturbances, and to determine the performance capability of the ASPS under these conditions. The most demanding and largest proposed payload, the Solar Optical Telescope (SOT), was selected for this study.

It was found that, in all cases, the ASPS more than satisfied the payload's requirements. It is therefore concluded that, to satisfy facility class payload requirements, the ASPS or a Shuttle orbiter free-drift mode (control system off) should be utilized.

INTRODUCTION

Projected Shuttle payloads for the 1980-1990 time period require pointing and stabilization far in excess of the Shuttle orbiter capabilities. In addition, these requirements must be satisfied for long viewing periods (up to one hour), and in the presence of carrier vehicle disturbances. The disturbances imparted to the vehicle are a result of crew activity or of vernier reaction control system (VRCS) thruster firings for orbiter attitude hold, in addition to the less severe orbital environment forces and torques. Some facility class payload developers have proposed the combined use of payload auxiliary pointing systems and image motion compensation (IMC) to satisfy these pointing and stability requirements.

A candidate auxiliary pointing system for these applications is the Annular Suspension and Pointing System (ASPS). The ASPS is composed of a

vernier subsystem, a gimbal subassembly, a digital controller, and associated electronics (references 1 and 2). Previous simulation studies of ASPS performed by Langley and JPL (references 1 and 3) have shown its applicability in satisfying the mission requirements of small experiments (up to 600 kg). However, since ASPS is designed for use by a large variety of payloads, it becomes necessary to establish its viability for facility-class instruments in the Shuttle orbiter disturbance environment. Preliminary analyses conducted by Sperry Flight Systems for the ASPS gimbal subsystem (AGS) to evaluate its performance under the disturbance conditions noted above indicated that the pointing and stability requirements of large payloads could not be satisfied during periods of single-axis VRCS firings. Therefore, an investigation was undertaken, using a multi-degree of freedom simulation of the ASPS, Shuttle orbiter, and payload, to define the performance of this pointing system with a large payload during periods of VRCS firings and crew motions.

SYMBOLS AND ABBREVIATIONS

$A_{\perp LOS}$	acceleration perpendicular to payload line of sight
A	"A" station of magnetic suspension system
B	"B" station of magnetic suspension system
C	"C" station of magnetic suspension system
T_Y	lateral gimbal torque
T_σ	elevation gimbal torque
U	"U" station of magnetic suspension system
V	"V" station of magnetic suspension system
W	roll motor station of vernier system
X, Y, Z	ASPS vernier assembly axes
X_E, Y_E, Z_E	ASPS elevation gimbal axes
X_L, Y_L, Z_L	ASPS lateral gimbal axes
X_P, Y_P, Z_P	payload axes
X_S, Y_S, Z_S	shuttle pitch, roll, and yaw axes, respectively

} Axial MBA's

} Radial MBA's

} See figure 4

x_{SOT} , y_{SOT} , z_{SOT}	SOT axes
γ	ASPS lateral gimbal angle
θ	yaw pointing error
σ	ASPS elevation gimbal angle
ϕ	pitch pointing error
ψ	roll pointing error
AFD	aft flight deck of Shuttle orbiter
AGS	ASPS gimbal subsystem
ASPS	Annular Suspension and Pointing System
AVS	ASPS vernier subsystem
BDC Torquer	brushless direct current torquer (figure 1)
DEA	digital electronics assembly
DRIRU-II	dry rotor inertial reference unit-II
GEA	gimbal electronics assembly
IMC	image motion compensation
JPL	Jet Propulsion Laboratory
LOS	line of sight
MBA	magnetic bearing actuator
NSSC-II	NASA standard spacecraft computer-II
PEA	payload electronics assembly
SOT	solar optical telescope
VEA	vernier electronics assembly
VRCS	vernier reaction control system for Shuttle orbiter

ASPS DESCRIPTION

The payload auxiliary pointing system utilized in this analysis is the Annular Suspension and Pointing System (ASPS). The ASPS, figure 1, is composed of the following major subassemblies:

- 1) Vernier Subassembly
- 2) Gimbal Subassembly
- 3) Digital Controller
- 4) Associated Electronics

A description of each of these is presented herein.

ASPS Vernier Subsystem.- This subassembly, shown in figures 2 and 3, consists of a payload plate attached to an L-shaped rotor. This combination is suspended on five magnetic bearing actuators (MBA's), three axial and two radial MBA's (figure 4). These MBA's are used to provide control of the rotor motion in three translational and two rotational degrees of freedom. These two rotations, about axes in the plane of the rotor, are defined as pitch and yaw. The axis system is defined in figure 4. The third degree of rotational freedom, about an axis perpendicular to the plane of the rotor, and designated roll, is controlled by a segmented AC induction motor. Position of the rotor in the MBA gaps is determined by proximeters, while a resolver is utilized to determine roll position. Since no contacting elements are used in the AVS, the payload attached to the payload plate possesses six degrees of freedom and is isolated from the Shuttle orbiter induced disturbances. Latches are provided in this assembly to lock down the vernier during launch and reentry, and to prevent excessive motions of the rotor which might result in damage to the roll motor or the MBA's. These latches also serve to tie down the vernier in case of an MBA failure, thus permitting continuation of the mission, at reduced performance levels, using the ASPS gimbals.

ASPS Gimbal Subsystem (AGS).- This subassembly (figure 1) is comprised of two conventional gimbals attached to a mast which provides the interface structure between the Shuttle orbiter integration platform and the gimbals. This mast also contains a jettison system to be used in case of emergencies and a separation mechanism to permit the unloading of the gimbal bearings from payload induced vibrational loads during launch and reentry.

The two gimbals (elevation and lateral) are used for system deployment from the caged position after attaining orbit, for target acquisition and tracking, slewing to a new target, and as a backup to permit continuation of the mission, at reduced performance levels, in case of a vernier subsystem failure.

Each gimbal uses a 33.9 Newton-meters brushless DC torquer commutated by

a 12-speed resolver. A single speed resolver is employed to determine gimbal angle. A flex capsule is used to carry power and signals across the rotating interface. Each torquer is equipped with a secondary winding which, in conjunction with an optical encoder, permits the stepping down of the pointing system and its payload into the caged configuration should the primary torquer windings become inoperable.

Digital Controller.- Control of the ASPS is effected through the use of an NASA Standard Spacecraft Computer-II (NSSC-II), appropriate software, and associated conversion equipment. This digital approach has been selected to permit changes in system software during flight, thus allowing for fine tuning of the system performance, and to facilitate change-over between missions by relegating the input of payload or mission unique parameters to simple software changes.

The software associated with the pointing system has been modularized, thus providing maximum system flexibility to accommodate payload or mission changes, as well as pointing system configuration alterations as might be seen when flying the system without the vernier.

The software associated with the ASPS consists of the following modules: attitude control, attitude determination, mode control, sensor processing, failure monitoring and reporting, collision avoidance, command processing, display and telemetry, real-time executive, as well as some required utility program. Only those that were germane to this analysis were modeled.

Electronics.- A number of electronics assemblies are employed in the ASPS. The major assemblies are: the digital electronics assembly (DEA), the gimbal electronics assembly (GEA), the vernier electronics assembly (VEA), and the payload electronics assembly (PEA). The DEA provides the total interface between the ASPS computer (the NSSC-II) and the rest of the ASPS hardware, as well as the outside world. The GEA and VEA contain the control and driver electronics for the gimbal and vernier subassemblies, respectively. The PEA, located on the ASPS payload plate, provides the interface between ASPS and its sensor complement, such as the DRIRU-II gyro package.

A more complete description of the ASPS design and its development is presented in references 1 and 2.

PAYLOAD DESCRIPTION

Previous studies of this device considered its applicability only to small payloads (up to 600 kg). However, since ASPS is intended for use with a large variety of payloads, it was desired to verify the system's performance when applied to large payloads. It was therefore decided that the characteristics of the largest proposed payload would be utilized in this investigation. The largest known contemplated payload, to date, is the Solar Optical Telescope (SOT) being currently developed by the Goddard Space Flight Center.

From reference 4, the justification for this payload is that there exists "the need to achieve the very high spatial resolution required to determine the density, temperature, magnetic field, and nonthermal velocity field in a large number of solar features, on the scale of which the various physical processes of interest are occurring." To permit the attainment of these scientific goals, the SOT will evolve into an observing facility for Solar Physics. The configuration used in this analysis is shown in figure 5 and consists of a semi-monocoque truss structure 3.8 meters in diameter and 7.3 meters long. At the aft end of the truss structure is mounted a 1.25 meter aperture primary mirror weighing 700-800 kg. In addition to the primary instrument, there are also three major co-observing instrument facilities, along with three rotate-in and three swing-in cannisters, fed by the SOT primary mirror. The mass of this configuration is 6600 kg. The mass and inertia properties of this configuration, along with the pointing control and stability requirements are obtained from reference 5 and presented in table 1.

The SOT is currently being defined with the philosophy that the payload pointing system need only provide arcsecond stability while the telescope primary mirror assembly will satisfy the requirements for sub-arcsecond stability, alignment control, rastering, and IMC. This analysis did not subscribe to that approach. It was stipulated that the telescope would require mirror motions for focusing purposes only. However, all other control functions, such as fine pointing, would be performed by the ASPS.

SHUTTLE ORBITER VRCS

Because of orbital environment disturbances, as well as motions of the crew and payload equipment located in the bay, active control in the form of a reaction control system is utilized by the Shuttle orbiter to maintain attitude. Since control system activation cannot be readily predicted, it is imperative that the payload pointing system such as ASPS, be capable of maintaining payload pointing and stability during control thruster firings.

The vernier reaction control system (VRCS) configuration and characteristics for the Shuttle orbiter are shown in figure 6. This information represents a portion of the disturbance model used in this analysis and is identical to that employed by JPL (reference 3) and Sperry in previous pointing system studies.

ASPS performance was evaluated under various combinations of disturbances, resulting from VRCS firings and crew motions, in an attempt to identify the operational capability of the system under worst case conditions.

ANALYSIS CONDITIONS

The performance of the ASPS, with an SOT size payload, mounted in the

Shuttle orbiter payload bay was evaluated to establish the impact of the external disturbances on the system during periods of payload observations, when stringent control requirements must be satisfied. The analysis tool employed in this effort is a digital, multi-degree-of-freedom simulation of the ASPS, its payload, and the Shuttle orbiter, developed by the Langley Research Center.

This simulation encompasses the rigid body dynamics of the orbiter, the pointing system, and the payload, as well as mathematical models of various components of the system, such as magnetic bearing actuators, gimbal torquers, sensors, and digital controller, based on actual hardware data. Thus, this simulation is a high-fidelity representation of the hardware and should, therefore, be indicative of the performance of the system in its operational environment. No moving payload parts were simulated in this analysis.

For this effort, it was assumed that the ASPS and its payload, the SOT, were located aft and above the Shuttle center of mass as follows:

$$Y_S = 2.2 \text{ meters aft of Shuttle c.m.}$$

$$Z_S = 0.75 \text{ meters above Shuttle c.m.}$$

The Shuttle orbiter VRCS thrusters were distributed as shown in figure 6. Using this simulation, a survey was conducted to identify which combination of VRCS thruster firings and pointing system gimbal orientations resulted in the maximum acceleration on the payload. This would thus place maximum demands on the pointer's control system.

ASPS response to crew motions was also examined. A wall push-off by a crew-member located in the Shuttle aft flight deck (AFD) was used as the maximum disturbance (ref. 3). This represented a force of 100 Newtons. The crew member was assumed to be located, with respect to the orbiter center of mass, at the following coordinates:

$$X_S = 0.5 \text{ meters to the side of the orbiter c.m.}$$

$$Y_S = 16 \text{ meters forward of the orbiter c.m.}$$

$$Z_S = 0.5 \text{ meters above the orbiter c.m.}$$

Impact of crew motions in combination with VRCS firings about the pitch and roll axes, respectively, were examined. In the case of the pitch axis, the crew motion and VRCS firing were such that in one case the resultant translational accelerations along the Shuttle Z-axis were additive while moments about the Shuttle X-axis were counteracting. In the other condition, the direction of the crew motion was changed such that both the accelerations and moments were additive. For the roll axis disturbances, the resultant accelerations and moments were additive. In all cases, the standard VRCS firing times were maintained, even though, in reality for the all-additive conditions, the required burn time to effect the necessary

attitude correction with the thrusters would most likely be less than that simulated in this study.

Simultaneous, multi-axis attitude corrections with the VRCS were not evaluated in this study. Utilization of the VRCS for multi-axis control is included in the functional subsystem software requirements (reference 6). This software will be so structured as to select a combination of thrusters such that no more than three jets will be activated during a firing period. It is conceivable that certain combinations of three jets can be selected which will produce higher disturbances on the payload than those utilized in this analysis. However, from work performed at JSC on the evolution of this VRCS software, it has been determined that selection of such combinations by the logic is extremely remote. Therefore, based on currently available information, it appears that, for realistic combinations of three thrusters, the acceleration component along any one vehicle axis resulting from a multi-axis correction will be of no greater magnitude than the values used in this analysis.

Throughout this effort, the performance requirements placed on the ASPS were to satisfy the payload's, in this case the SOT, pointing and stability requirements even during periods of VRCS firings and crew movement.

ANALYSIS RESULTS

It became essential to define the worst case gimbal orientations of the pointer, or payload look-angle, for each firing condition, and to evaluate the system's performance in these orientations and under those disturbance conditions. The survey indicated that the maximum disturbances resulted from a pitch or roll axis VRCS firing. A scan was performed for various combinations of ASPS elevation and lateral gimbal angles for a pitch and a roll VRCS disturbance, individually. Preliminary studies indicated that the worst gimbal orientations existed in the range of σ (elevation gimbal angle) 0° to -90° and γ (lateral gimbal angle) from 0° to -60° . Although the worst case angles may be more closely determined, the entire range is shown to indicate trends. The results of the survey task are presented in figures 7-18. The data presented in figures 7 through 12, for a pitch disturbance, and 13 through 18, for a roll disturbance, indicate the maximum value of several parameters for various combination of gimbal angles. These parameters include: maximum acceleration perpendicular to the payload LOS (Z_p in figure 4) measured at the lateral gimbal center of mass and at the payload/payload mounting place center of mass (on the isolated side of the AVS); maximum required axial and radial MBA forces; maximum roll motor force tangent to the vernier system rotor; maximum required lateral and elevation gimbal torques; and maximum resultant payload pointing errors in pitch, yaw, and roll, respectively. To improve the resolution in the data for the roll VRCS disturbance, the axes of presentation for σ and γ were reversed.

It can readily be noted from figures 7 and 8, for pitch, as well as 13 and 14, for roll, that the vernier provides excellent isolation of the

payload from the carrier vehicle disturbance (note scale change between figures 7 and 8, as well as between 13 and 14). The maximum acceleration perpendicular to the LOS is at least an order of magnitude smaller on the payload side (figure 8 and 14) of the vernier than on the gimbal side (figures 7 and 13).

To combat these disturbance levels, the MBA's, the roll motor, and the gimbal torquers, must generate appropriate forces and torques. The ASPS actuators, to date, have been designed and manufactured with the following capacity:

Elevation and Lateral Gimbal Torquers	33.9 N-m each
Axial MBA's	33.4 N each
Radial MBA's	14.2 N each
Roll Motor	1.9 N

As can be seen from figures 9, 10, and 11 (pitch disturbance), as well as 15, 16, and 17 (roll disturbance), the capacity limits of the vernier subsystem actuators, with the exception of a few cases for the roll motor (figure 10), were neither exceeded nor approached. The roll motor is currently under resizing study.

Figures 12 and 18, for the pitch and roll disturbance, respectively, demonstrate that the pointing requirements of the payload, defined in table 1, were, for all conditions, always satisfied. In addition, it can be noted that these errors never exceeded the pointing and stability goals (≈ 0.01 arcseconds) set for the ASPS at the onset of its development program.

ASPS performance while being subjected to crew motions, as well as to combined crew motion and VRCS firing disturbances, was also examined. The results of these tasks are presented in table 2. The gimbal angle conditions, or payload look-angles, selected for these cases were those which previously resulted in having the payload subjected to the maximum acceleration perpendicular to the payload LOS produced by either a pitch or roll VRCS disturbance.

Figures 19(a) through 19(d) depict the impact of a pitch axis VRCS firing on the ASPS and its payload in the form of time histories. These are typical system time histories and representative of the ASPS response to a VRCS-generated disturbance while supporting a large facility class payload such as SOT.

Since it is not currently possible for the Shuttle orbiter VRCS to provide on-axis firings in more than one axis at a time, because of the maximum three-jet limitation, it was decided to examine the case of consecutive firings about two individual axes. The time between firings was set at 3 milliseconds to allow for recharge of the system. It was felt that such conditions would be in keeping with the worst case condition

philosophy followed throughout this effort, and was a realistic potential condition. Therefore, a VRCS firing about the vehicle's pitch axis, immediately followed by one about the roll axis, was simulated. The results of this evaluation are also presented in table 2.

As can be seen from table 2, the maximum values of the salient system parameters, excluding the roll motor force, never exceeded the limits dictated by the payload requirements or the pointing system's capability.

CONCLUDING REMARKS

An analysis was conducted to determine the performance capability of the ASPS in satisfying facility-class payload requirements, such as those dictated by SOT for example. The ASPS and its payload were subjected to the disturbance environment of the orbiter including crew movements and VRCS thruster firings. Numerous disturbance conditions and combinations were examined in this analysis. In all of these cases the pointing requirements of the payload were met. Except in a few conditions for the roll motor (figure 10), capabilities were not exceeded. The simulation option used throughout this analysis included only rigid body dynamics of the Shuttle orbiter, the ASPS, and the payload (SOT), as well as ideal sensors. However, it is anticipated that inclusions of full system characteristics, such as sensor noise, will have little impact on system response, and conformance with system requirements is expected. Preliminary examinations of the impact of such hardware characteristics as sensor noise have shown an overall system performance reduction of less than 5 percent. Owing to these results, therefore, it is concluded that the ASPS can satisfy the mission requirements of facility class payloads, such as SOT, without restraining crew activity or requiring free-drift mode (turning off the VRCS) operation from the Shuttle. However, to ensure that SOT requirements can be satisfied for any conceivable gimbal orientation, the data from this analysis indicate that an increase in roll motor capability is justified.

REFERENCES

1. Anderson, W. W.; Groom, N. J.; and Woolley, C. T.: Annular Suspension and Pointing System. Article No. 78-1310R, Journal of Guidance and Control, Vol. 2, No. 5; September-October 1979.
2. Cunningham, D. C.; Gismondi, T. P.; and Wilson, G. W.: System Design of the Annular Suspension and Pointing System (ASPS). Paper presented at the AIAA Guidance and Control Conference, Palo Alto, CA; August 7-9, 1978.
3. Anon.: Space Shuttle Experiment Pointing Mount (EPM) Systems: An Evaluation of Concepts and Technologies. Vol. II, Technical Report; JPL Report 701-1; April 1, 1977.
4. Anon.: Solar Optical Telescope Program Plan, Executive Summary; Shuttle Spacelab Payloads Project Office, Goddard Space Flight Center; May 1978.
5. Meffe, M. E.: Study of Large Facility Class Payloads for AGS Application. Sperry report prepared under NASA Contract NAS1-15008; November 1978.
6. Anon.: Space Shuttle Orbiter Flight Test, Level C: Functional Subsystem Software Requirements, Guidance, Navigation, and Control; Part C: Flight Control, Orbit 2; Rockwell International Document SD76-SH-009A. Prepared under contract NAS9-14000; April 15, 1979.

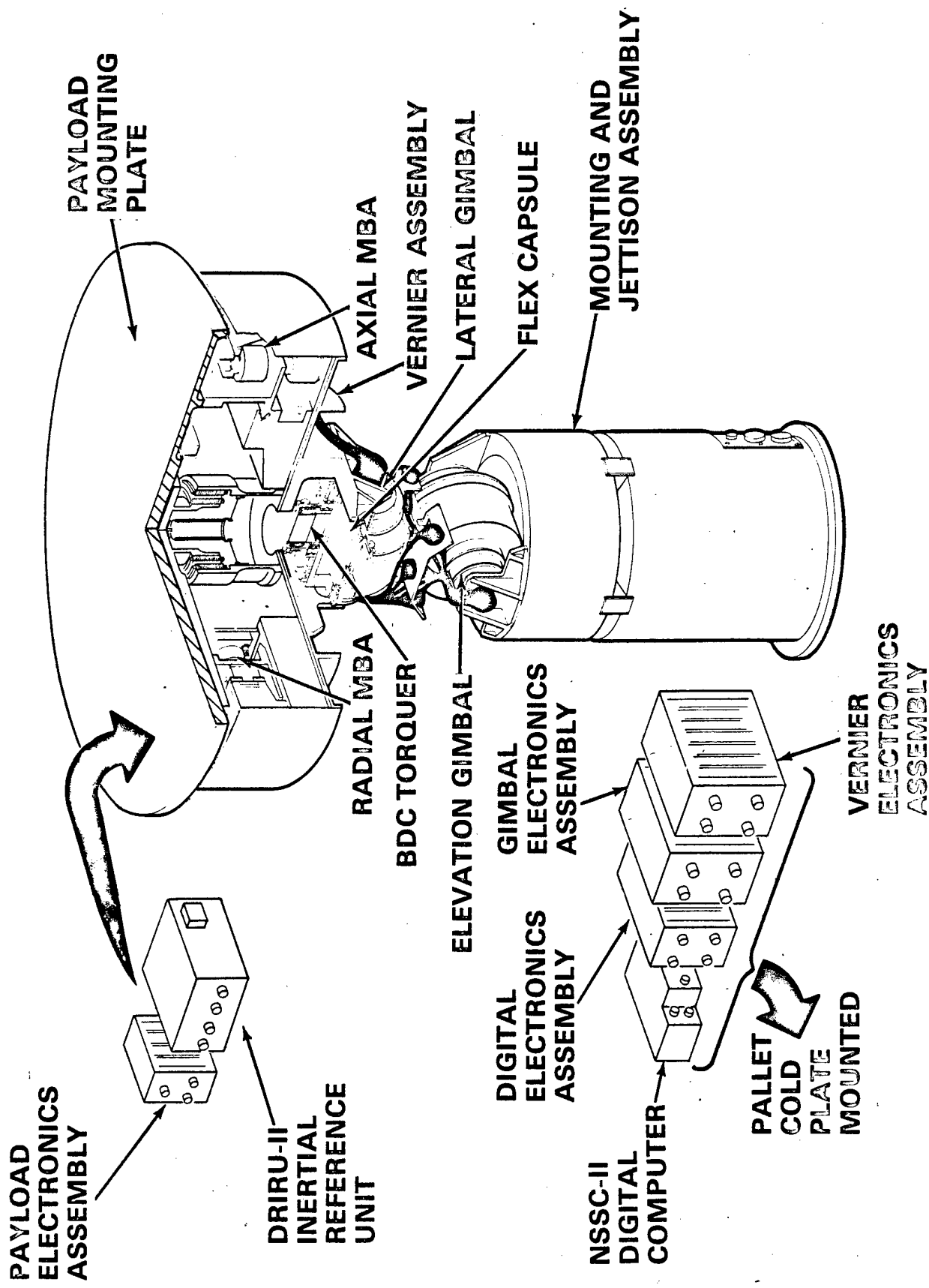


Figure 1.- Annular Suspension and Pointing System (ASPS) concept.

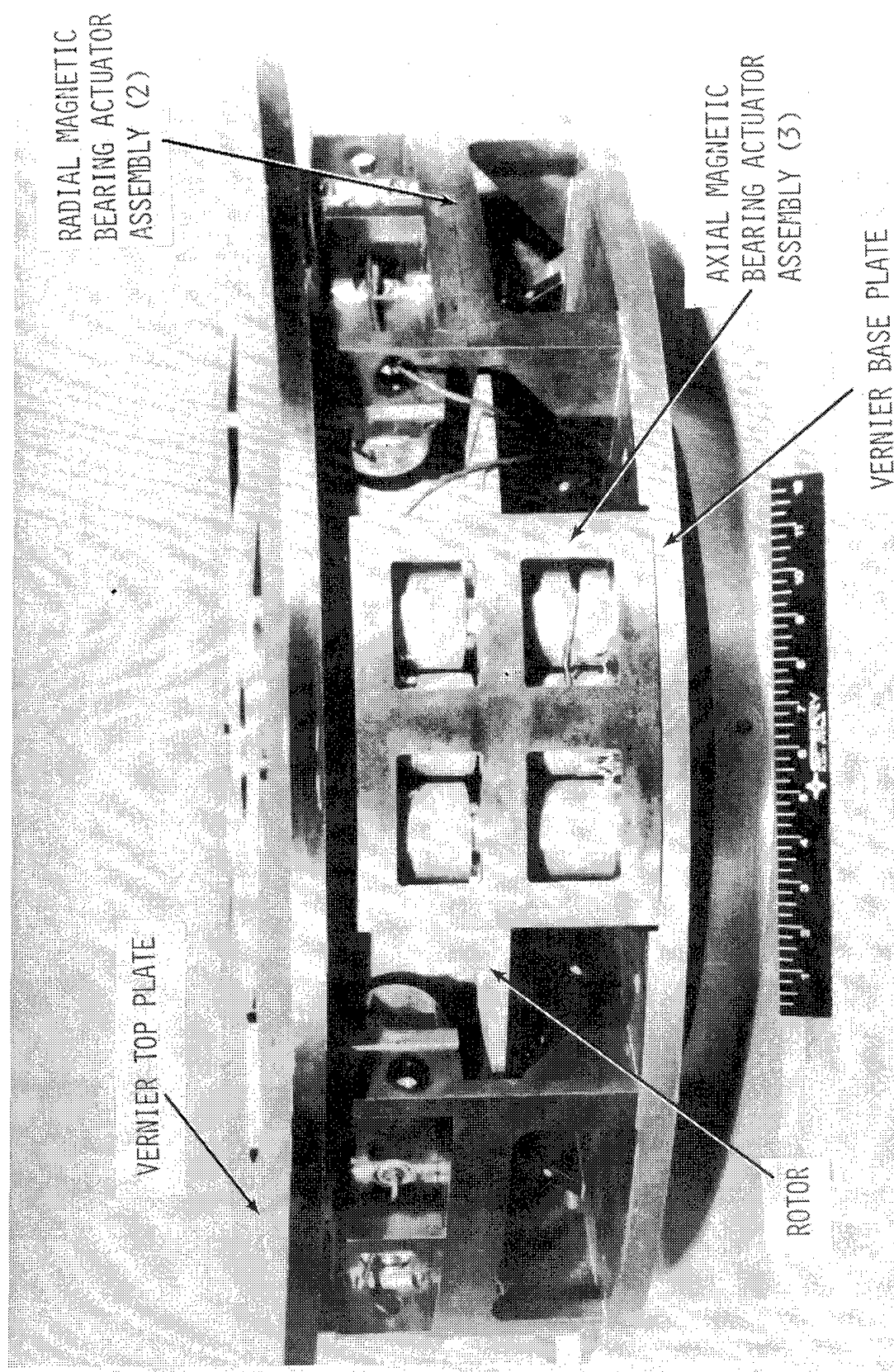


Figure 2. Side view of laboratory ASPS vernier assembly.

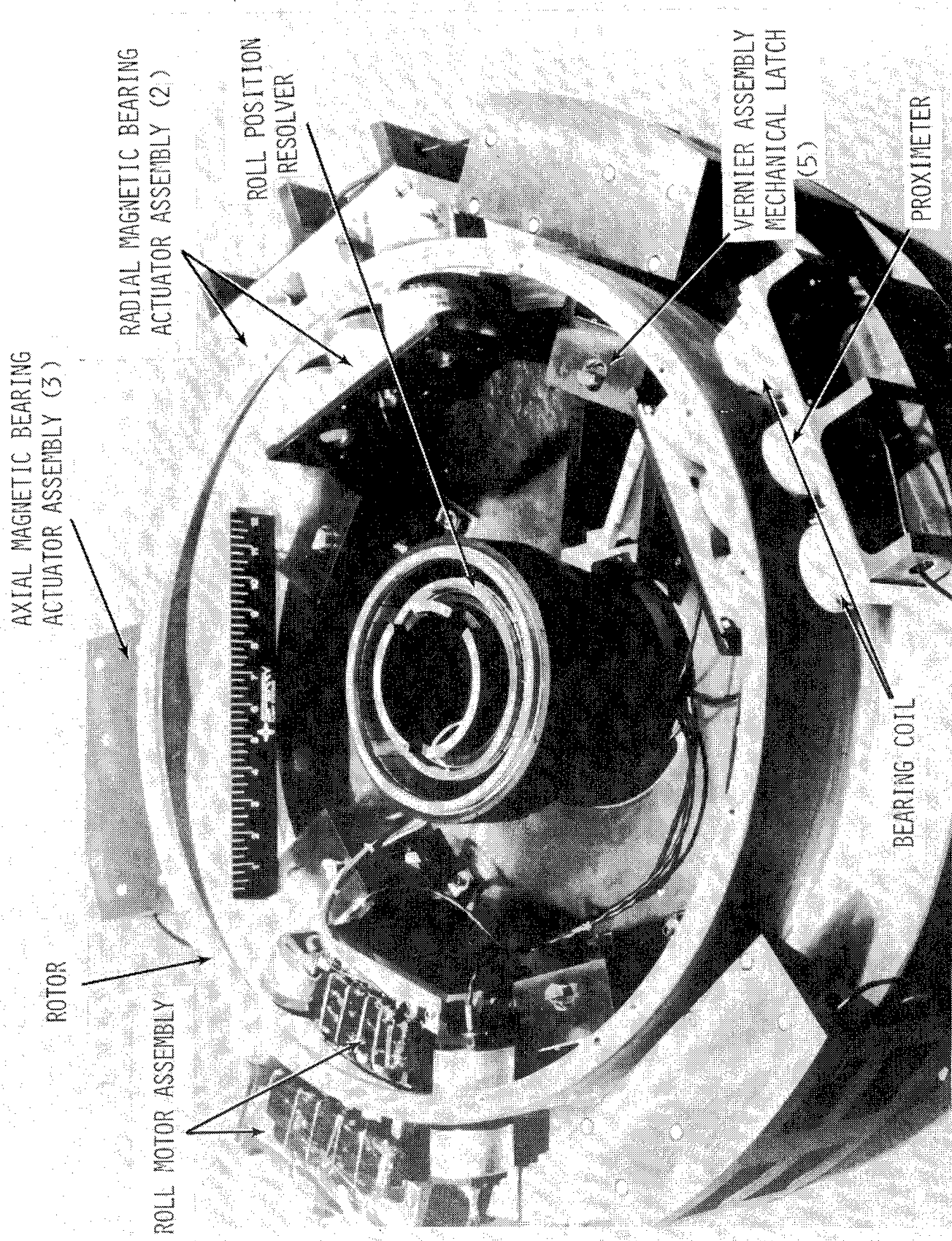


Figure 3.-Top internal view of laboratory ASPS vernier assembly.

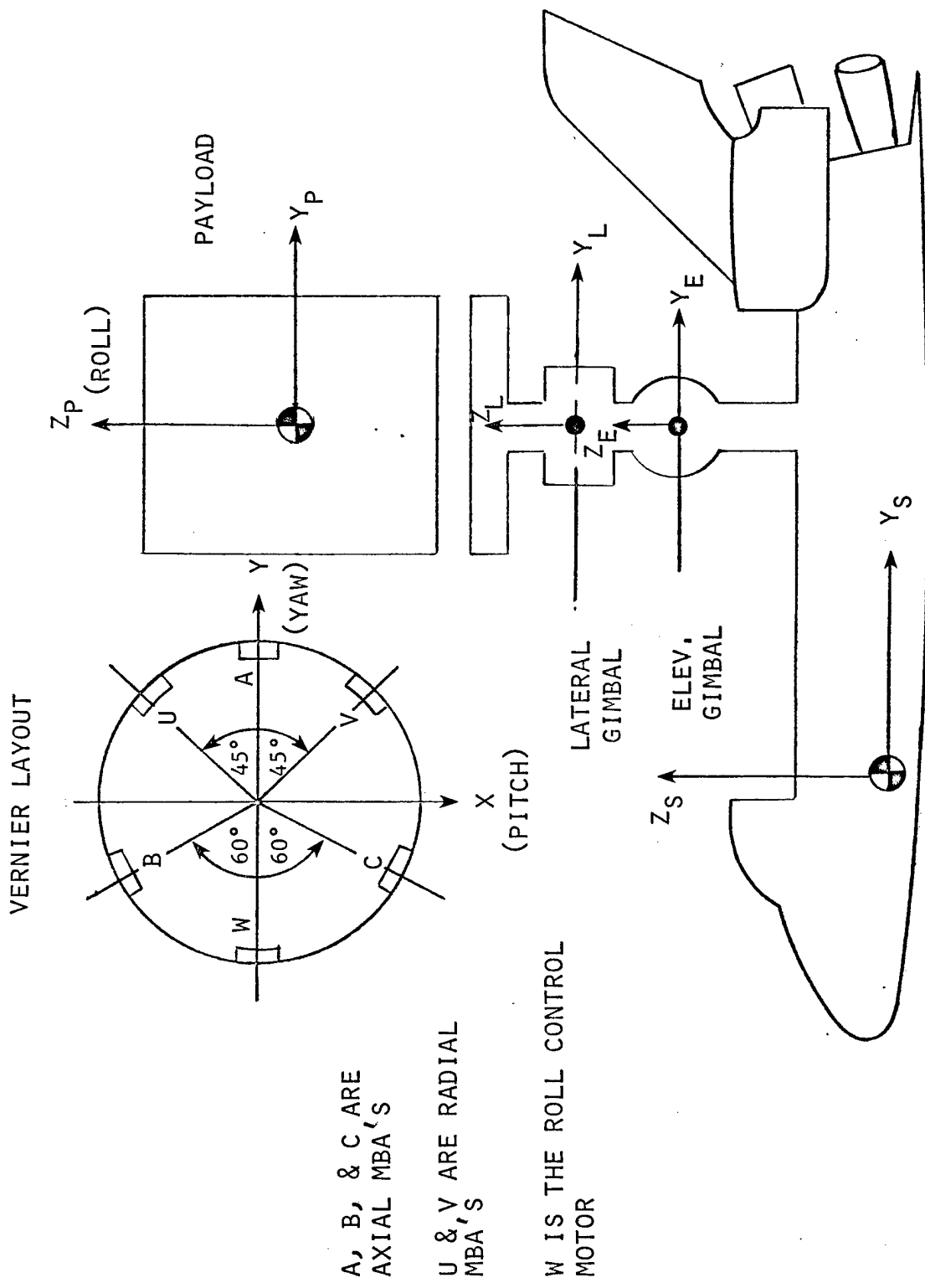


Figure 4.- Definition of coordinate systems.

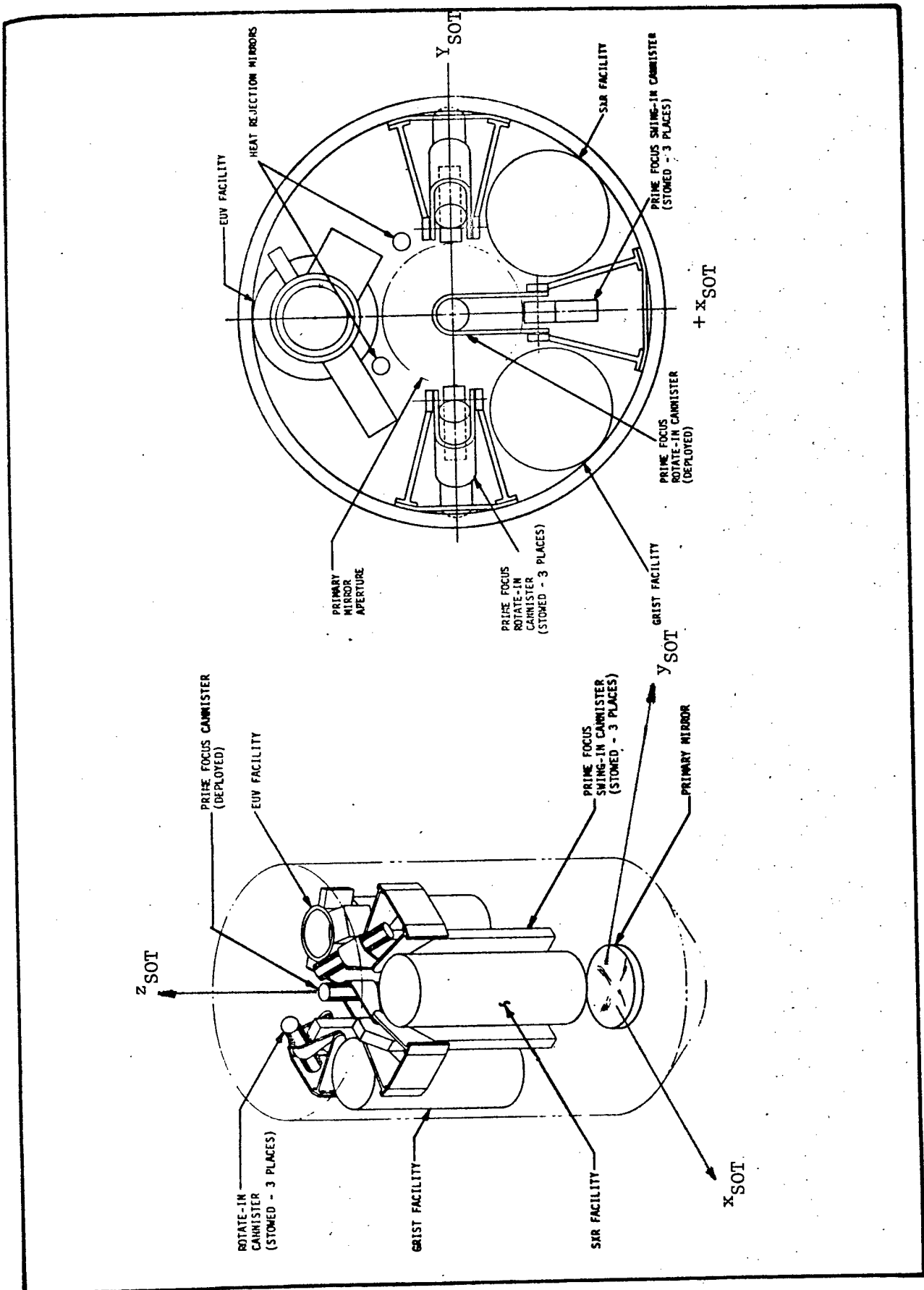
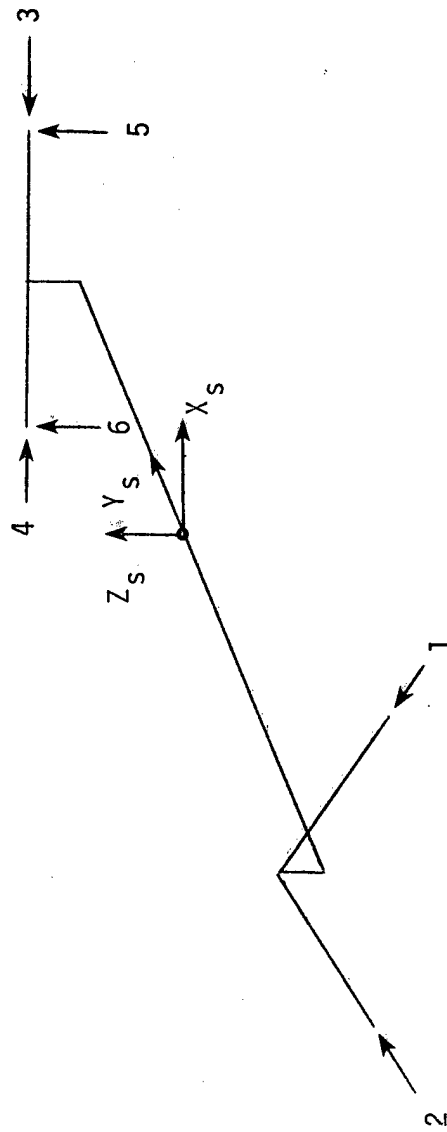


Figure 5.— Solar Optical Telescope (SOT) concept.

AXIS	BURN TIME (SEC)	VRCS ANGULAR ACCELERATION (RAD/SEC ²)	VRCS TRANSLATIONAL ACCELERATION (M/SEC ²)			THRUSTERS OPERATING
			\ddot{X}_s	\ddot{Y}_s	\ddot{Z}_s	
Y_s ROLL (+)	.20	+6.215E - 4	+0.002176	0	+0.002318	2, 4, 6
X_s PITCH (+)	.52	+2.918E - 4	0	0	+0.00263	5, 6
Z_s YAW (+)	.48	+2.920E - 4	-0.0004518	0	+0.001004	2, 3



NOTES: STS-1 mass properties

$$\text{mass} = 5790 \text{ slugs} = 84,562 \text{ kg}$$

$$I_x = 6.282 \text{ E} + 6 \text{ s1-ft}^2 = 8.524 \text{ E} + 6 \text{ kg-m}^2$$

$$I_y = 0.293 \text{ E} + 6 \text{ s1-ft}^2 = 1.098 \text{ E} + 6 \text{ kg-m}^2$$

$$I_z = 6.544 \text{ E} + 6 \text{ s1-ft}^2 = 8.879 \text{ E} + 6 \text{ kg-m}^2$$

Figure 6.- Shuttle VRCS configuration and characteristics.

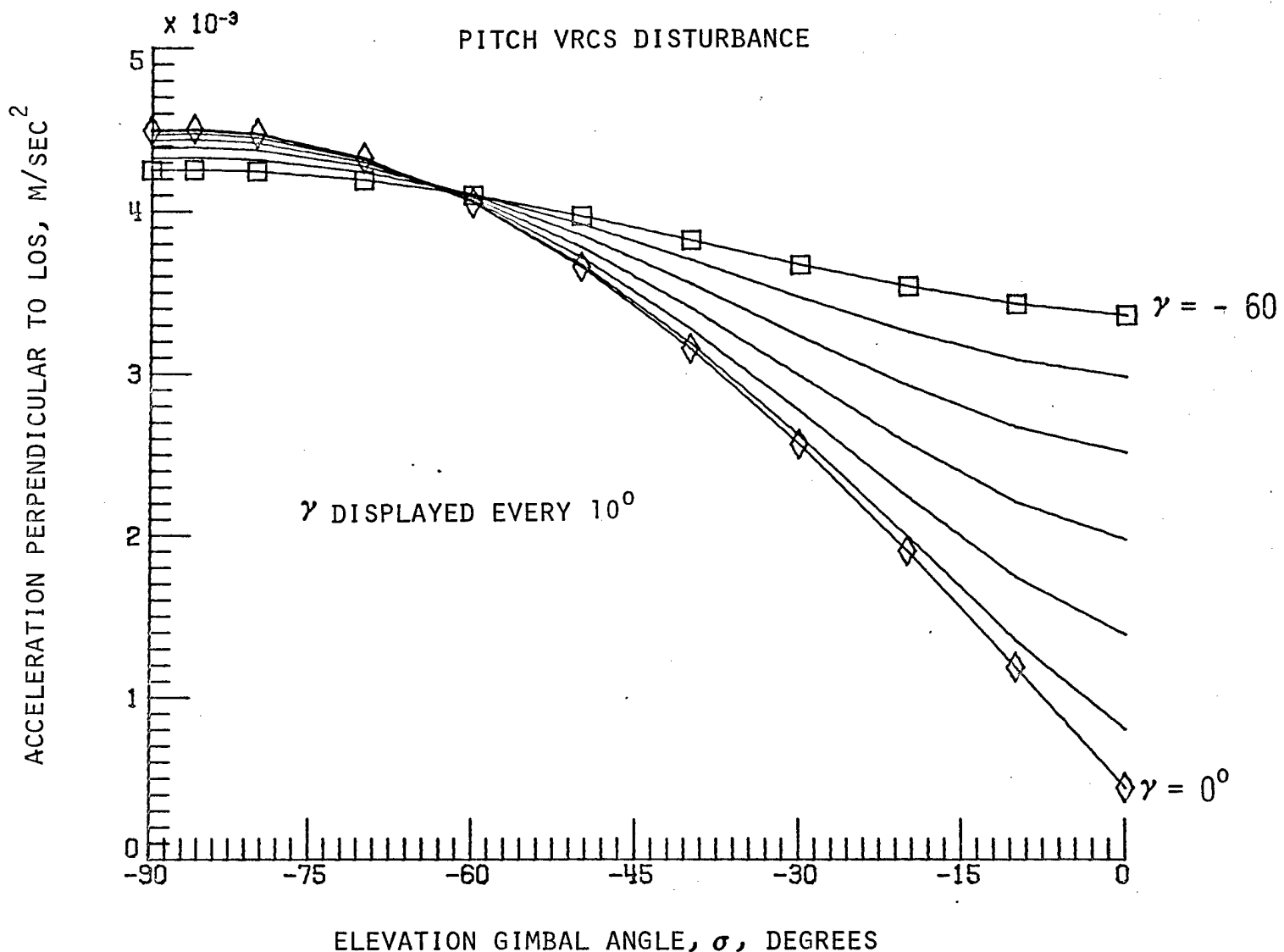


Figure 7.- Maximum acceleration perpendicular to the payload line-of-sight (LOS) measured at the lateral gimbal center of mass.

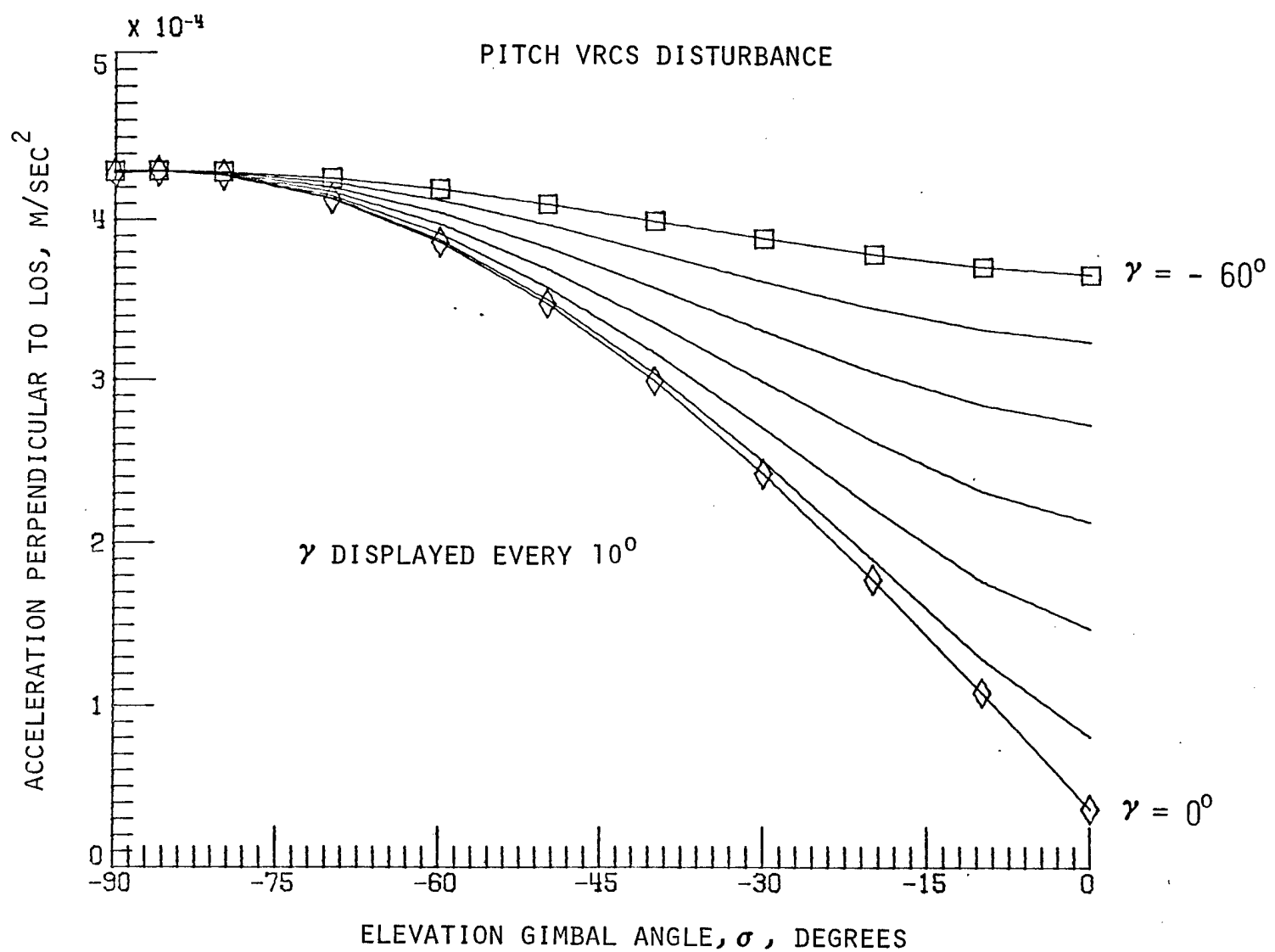


Figure 8.- Maximum acceleration perpendicular to the payload LOS measured at the payload/payload mounting plate center of mass.

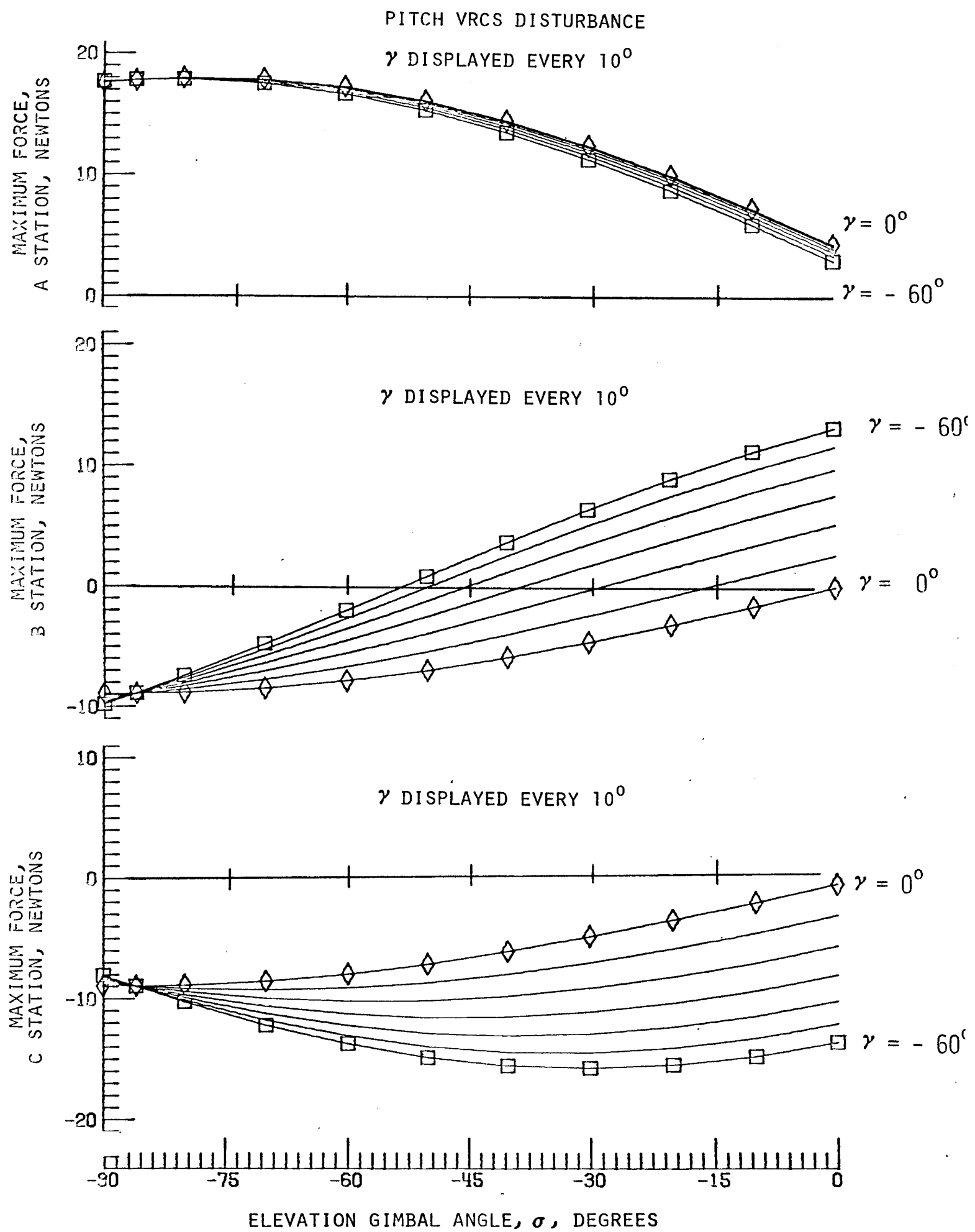


Figure 9.- Maximum axial MBA force for various payload look angles.

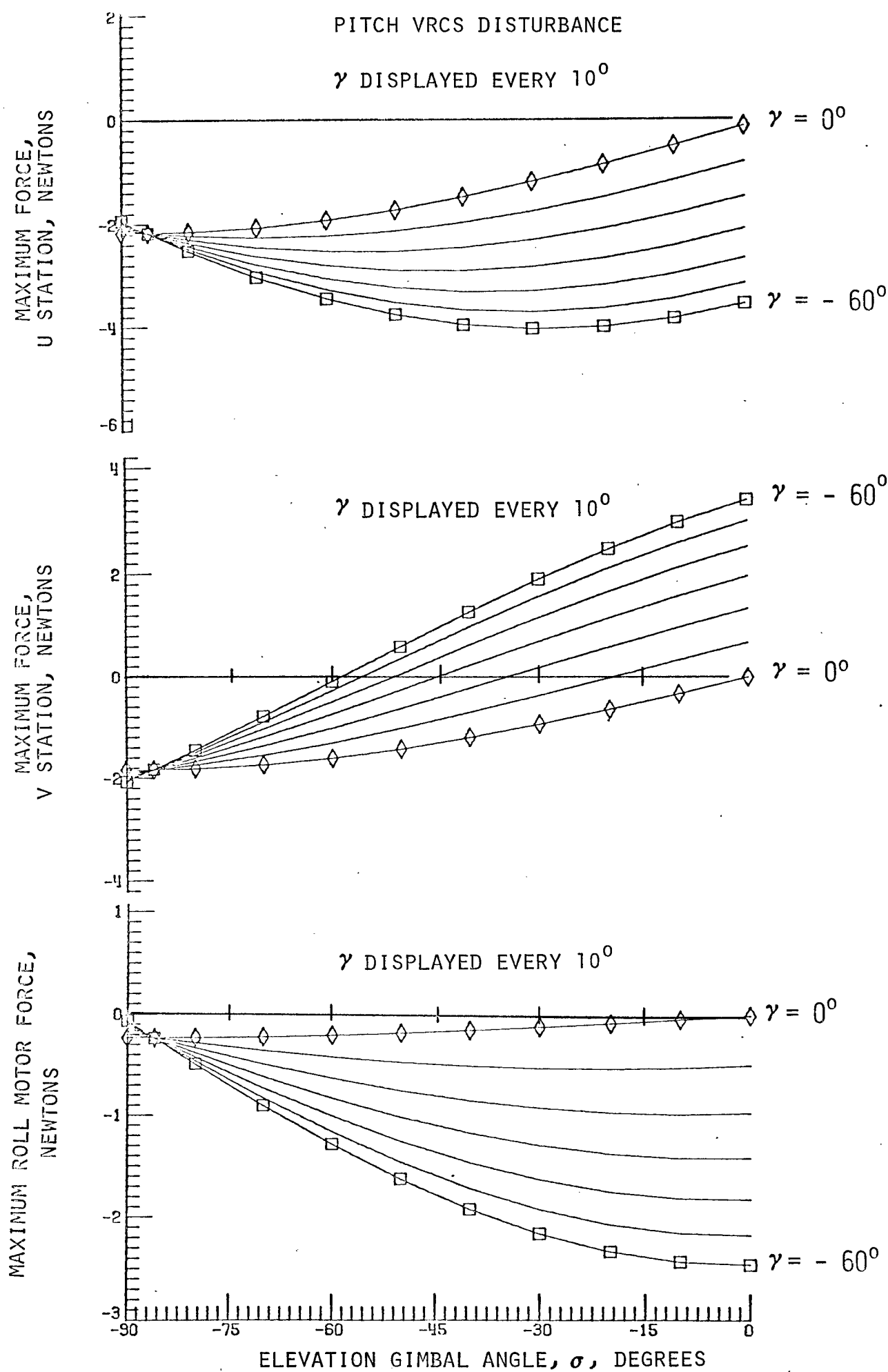


Figure 10.- Maximum radial MBA and roll motor force for various payload look angles.

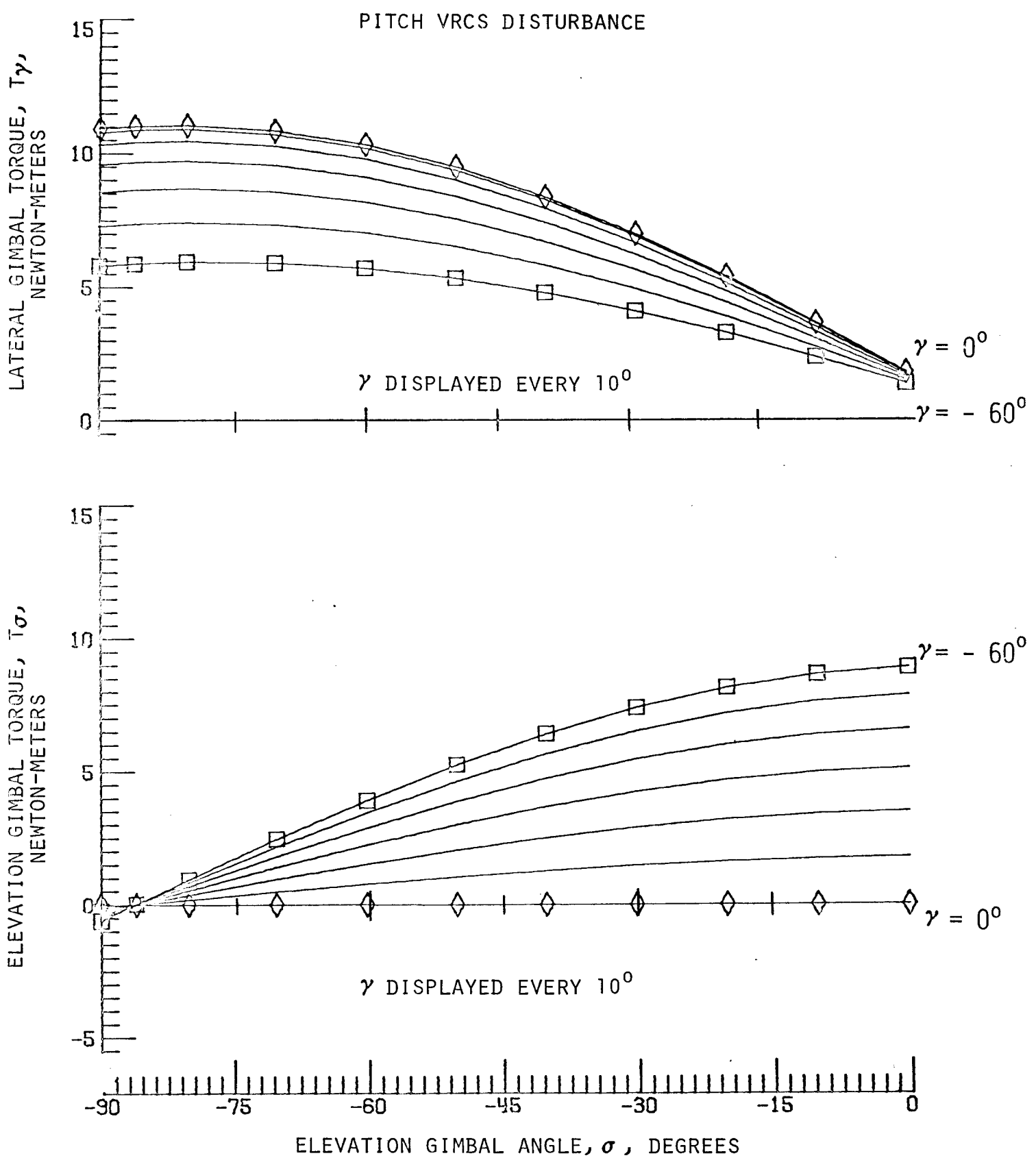


Figure 11.- Maximum gimbal torque for various payload look angles.

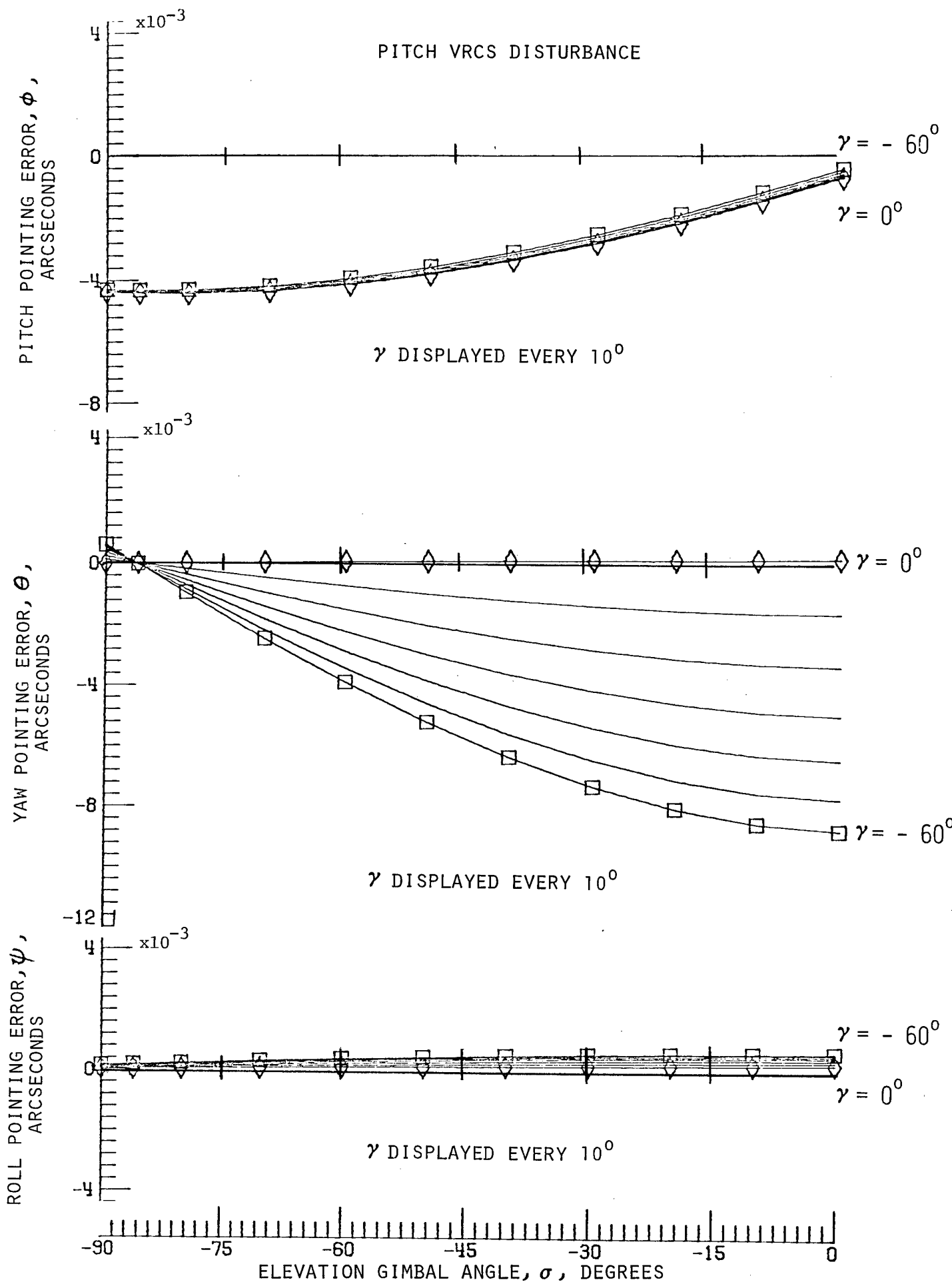


Figure 12.- Maximum payload pointing error for various payload look angles.

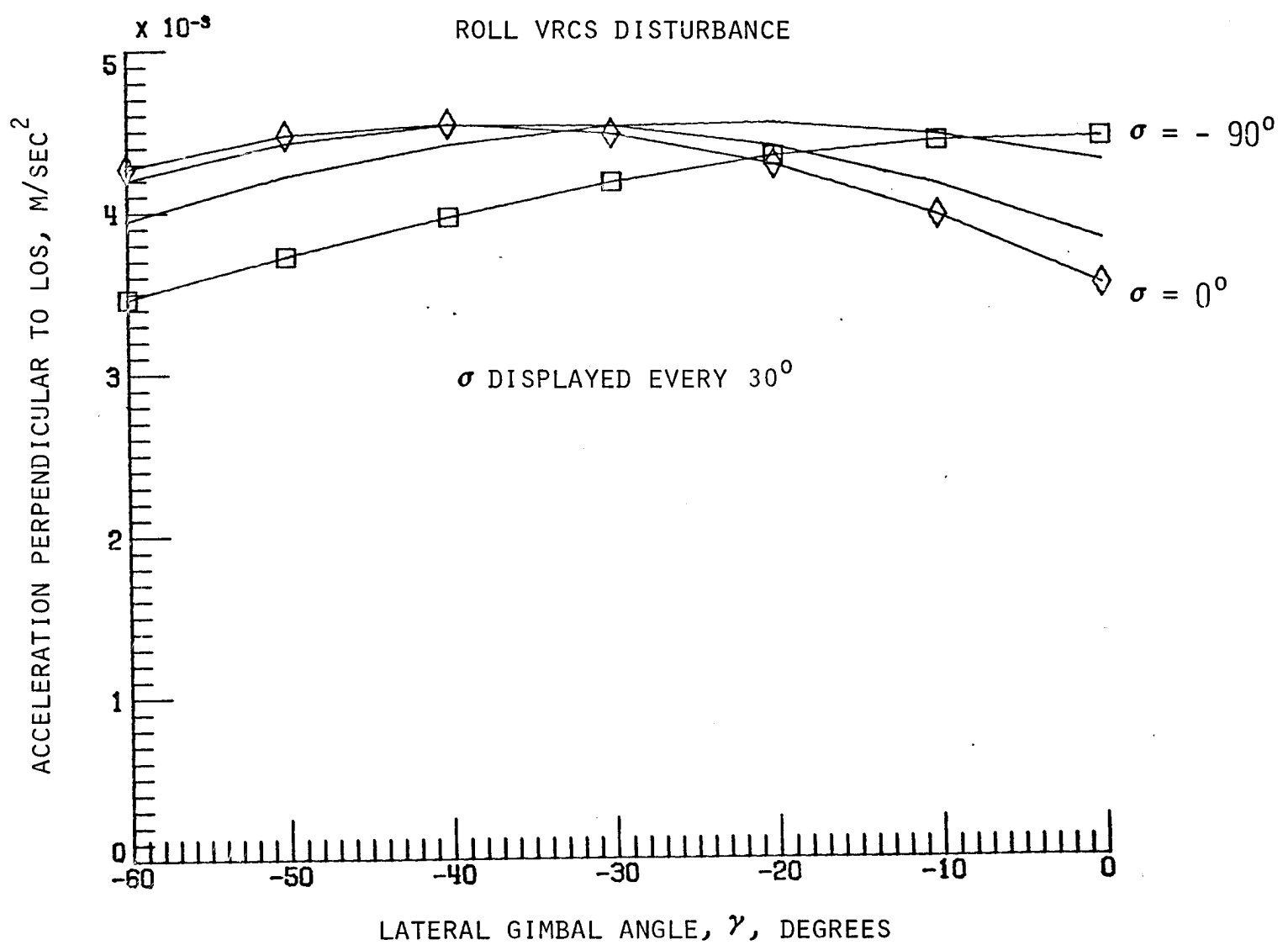


Figure 13.- Maximum acceleration perpendicular to the payload line-of-sight (LOS) measured at the lateral gimbal center of mass.

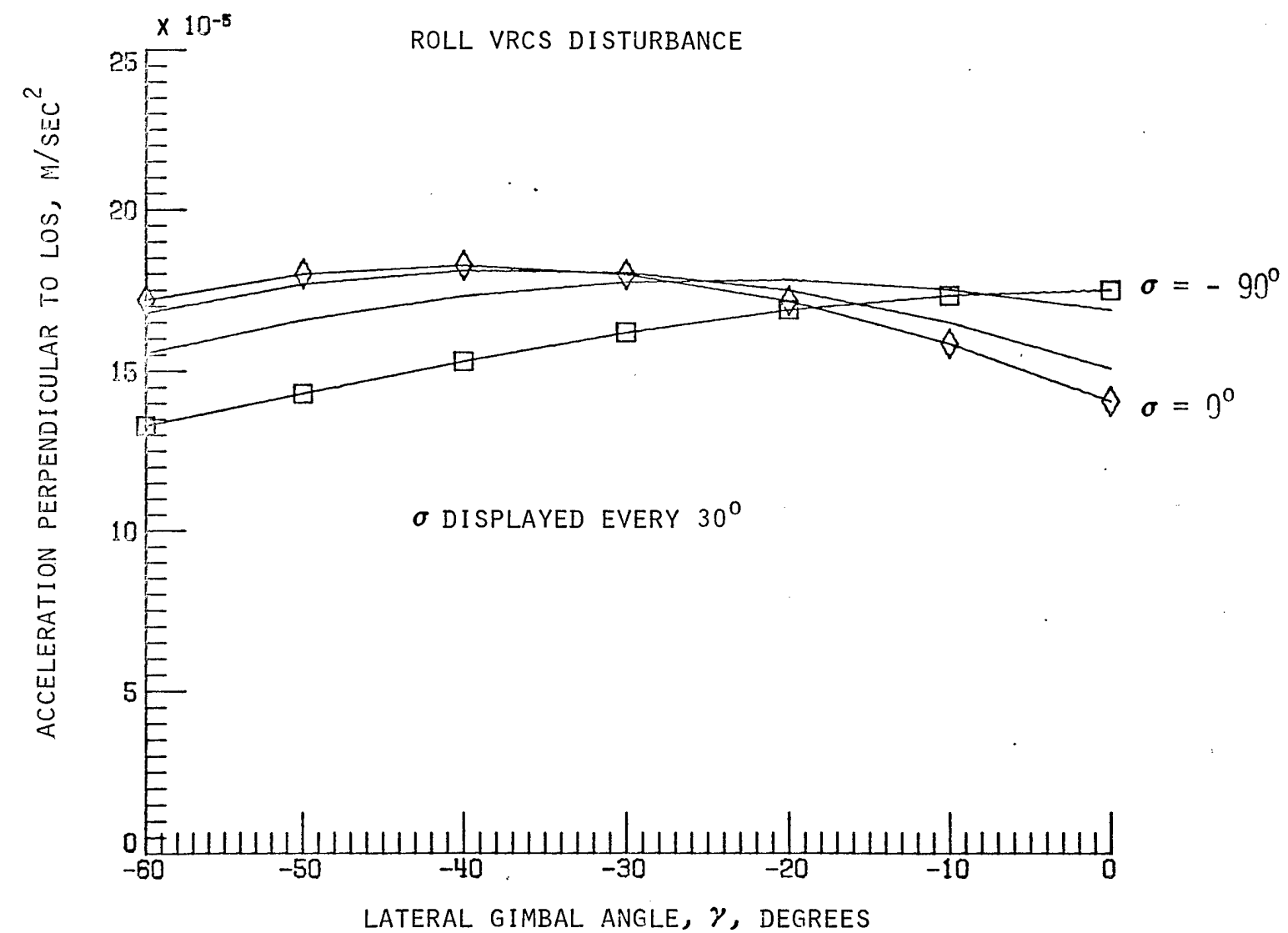


Figure 14.- Maximum acceleration perpendicular to the payload LOS measured at the payload/payload mounting plate center of mass.

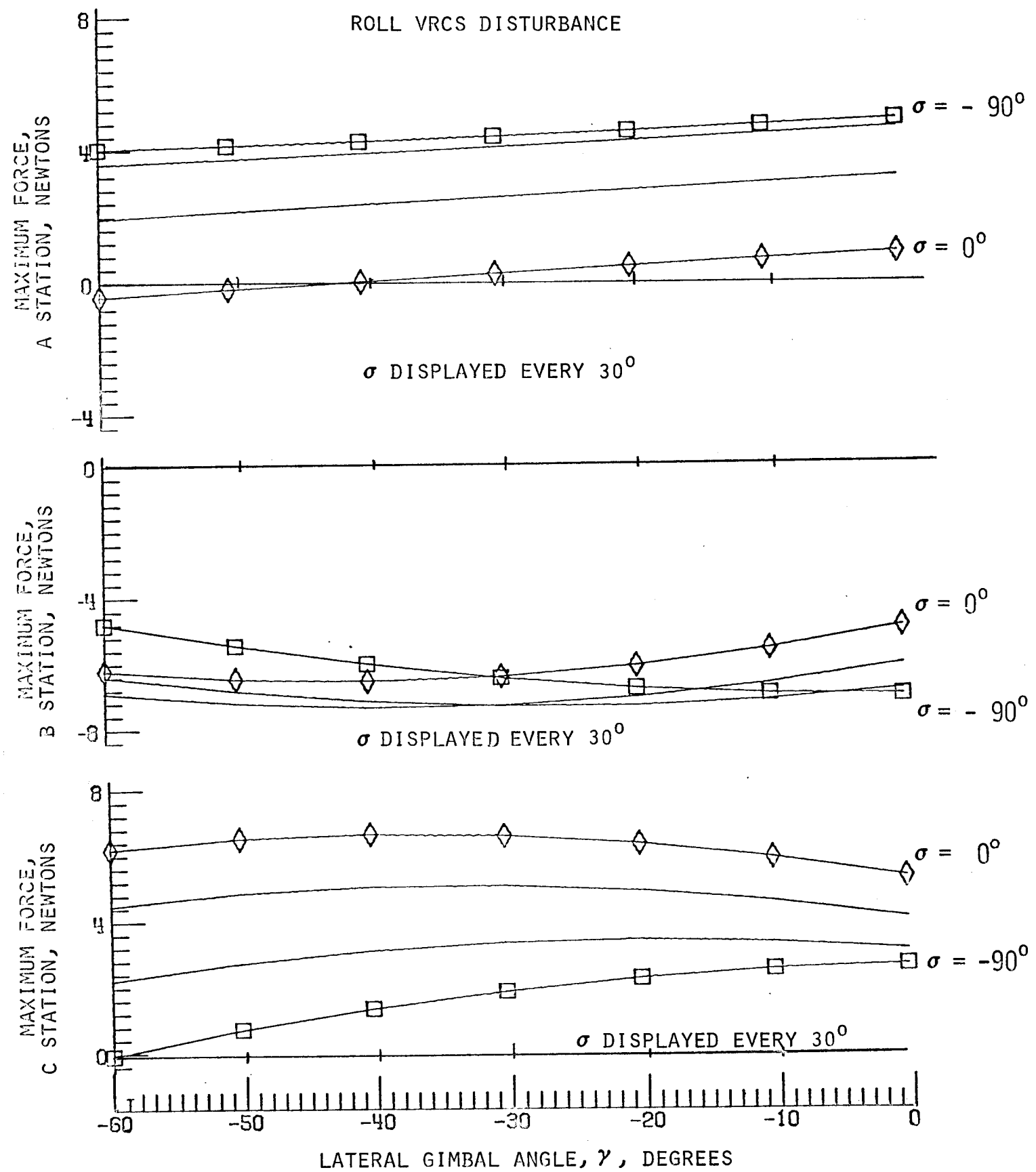


Figure 15.- Maximum axial MBA force for various payload look angles.

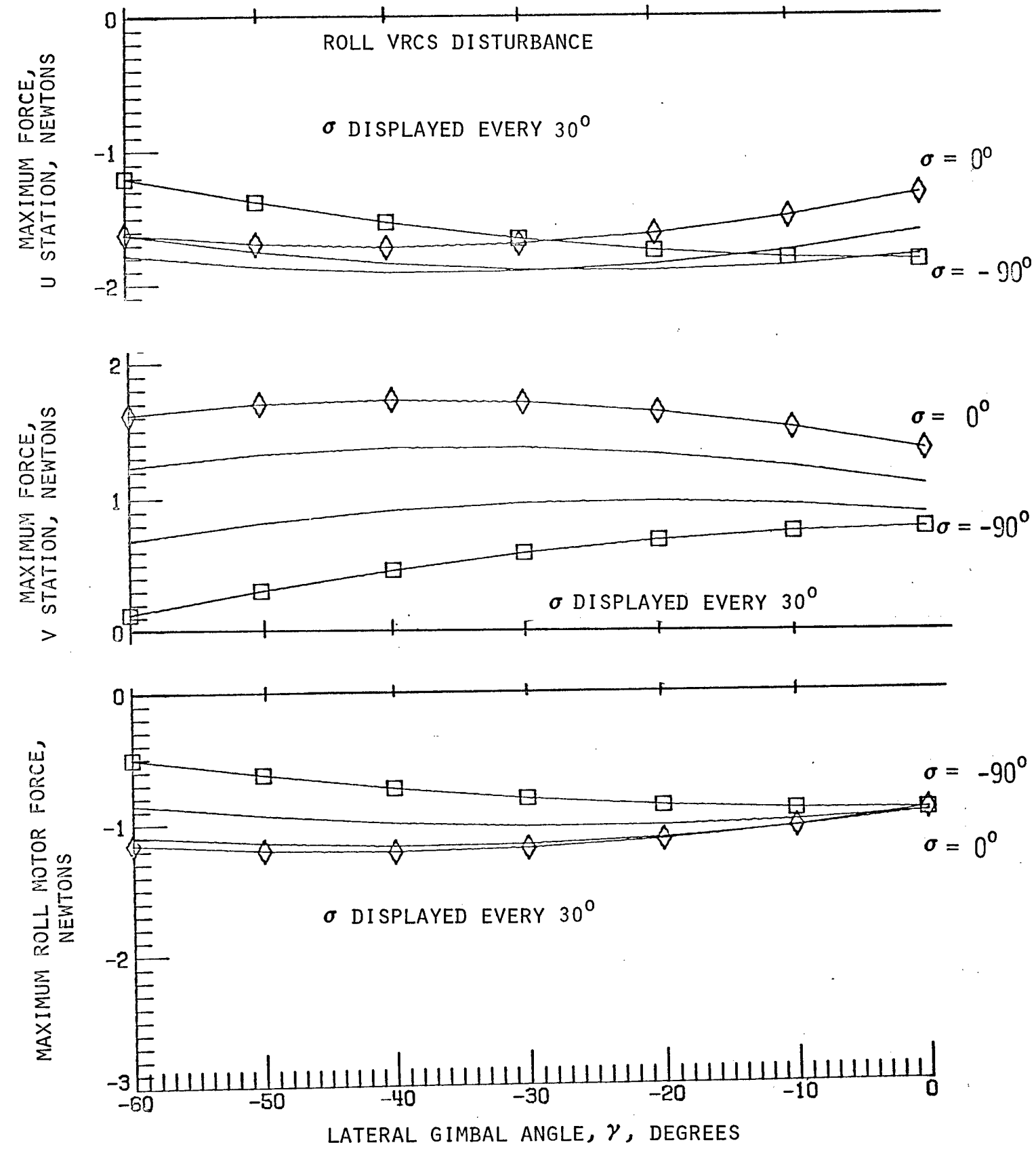


Figure 16.- Maximum radial MBA and roll motor force for various payload look angles.

ROLL VRCS DISTURBANCE

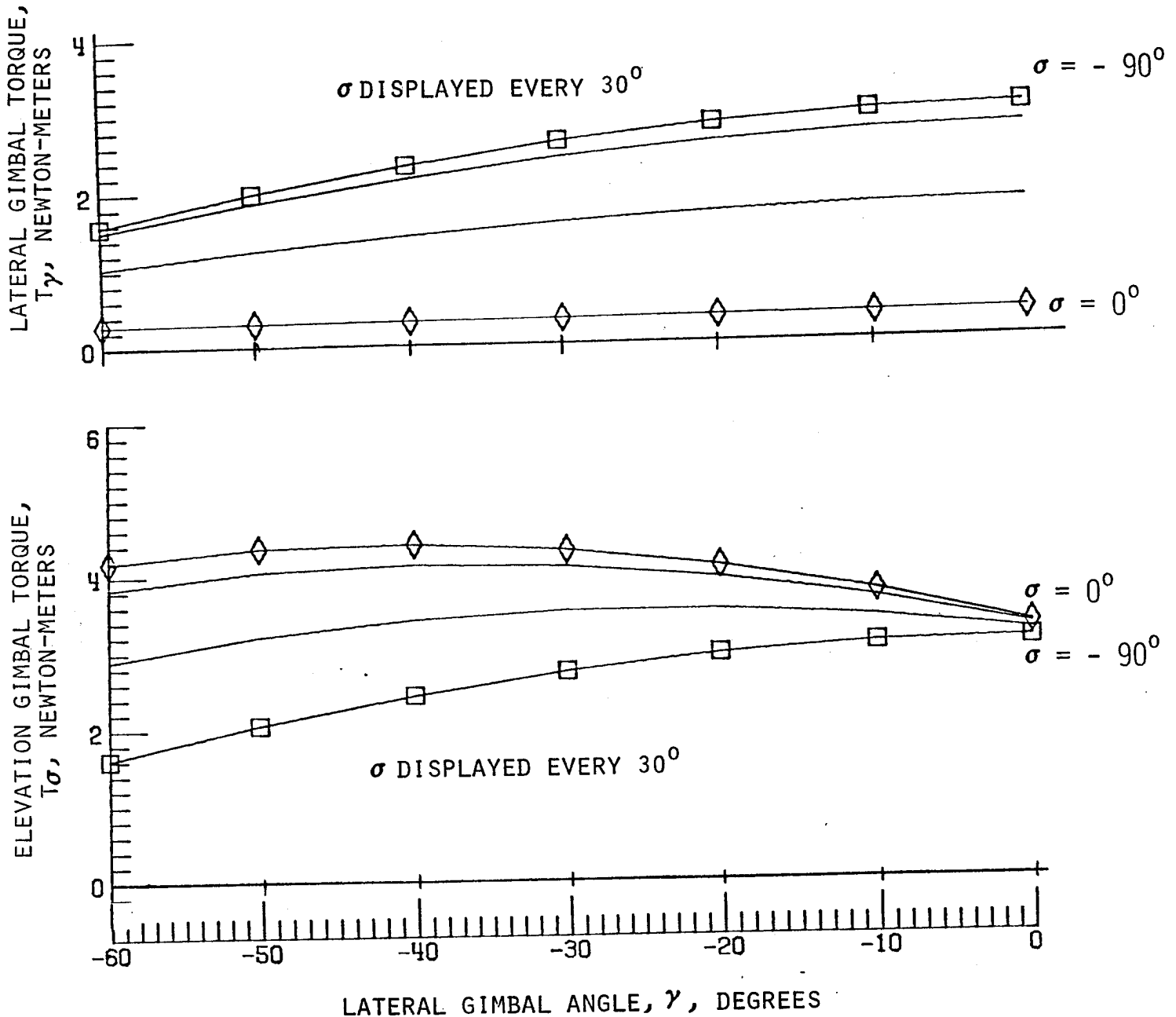


Figure 17.- Maximum gimbal torque for various payload look angles.

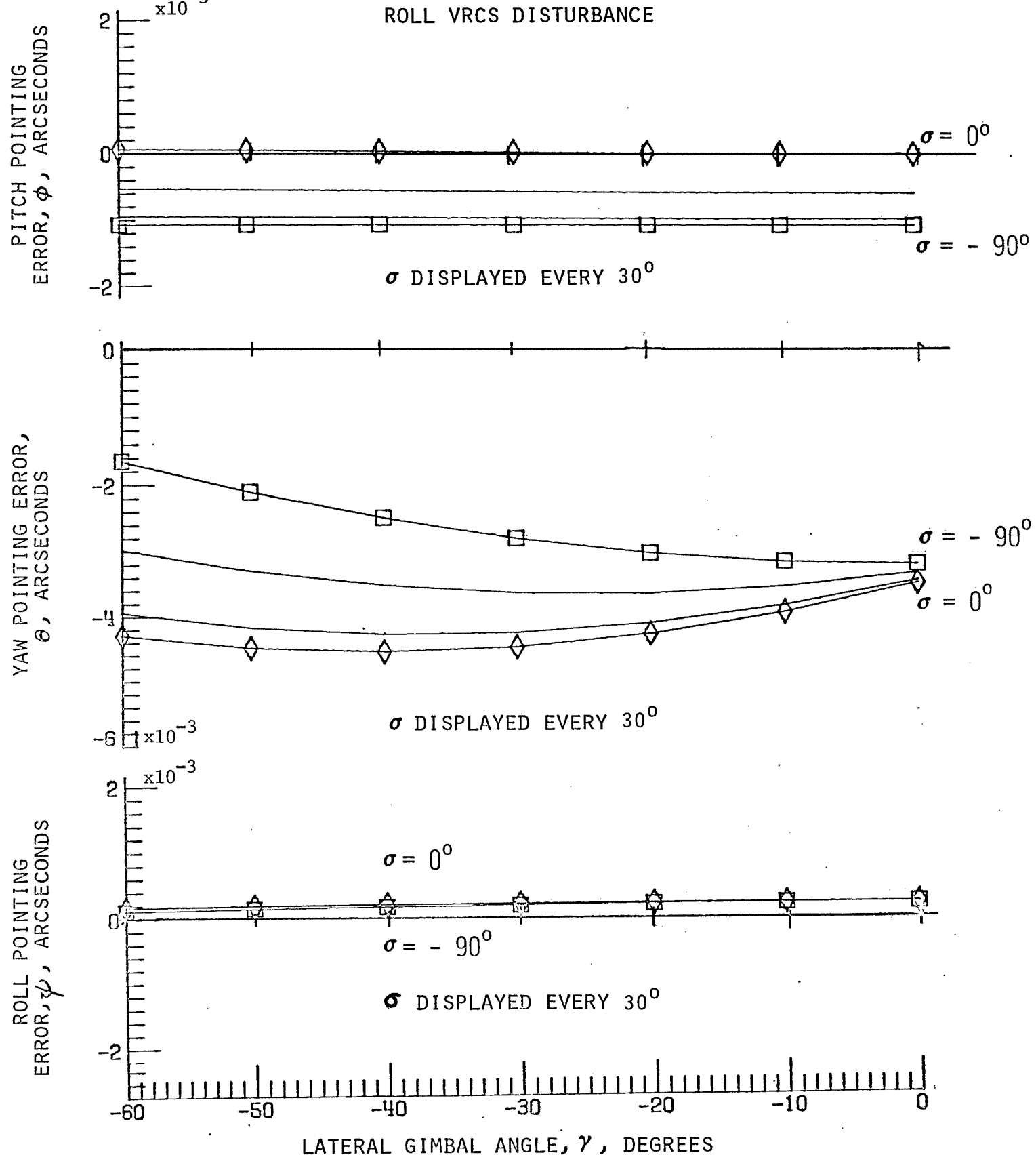


Figure 18.- Maximum payload pointing error for various payload look angles.

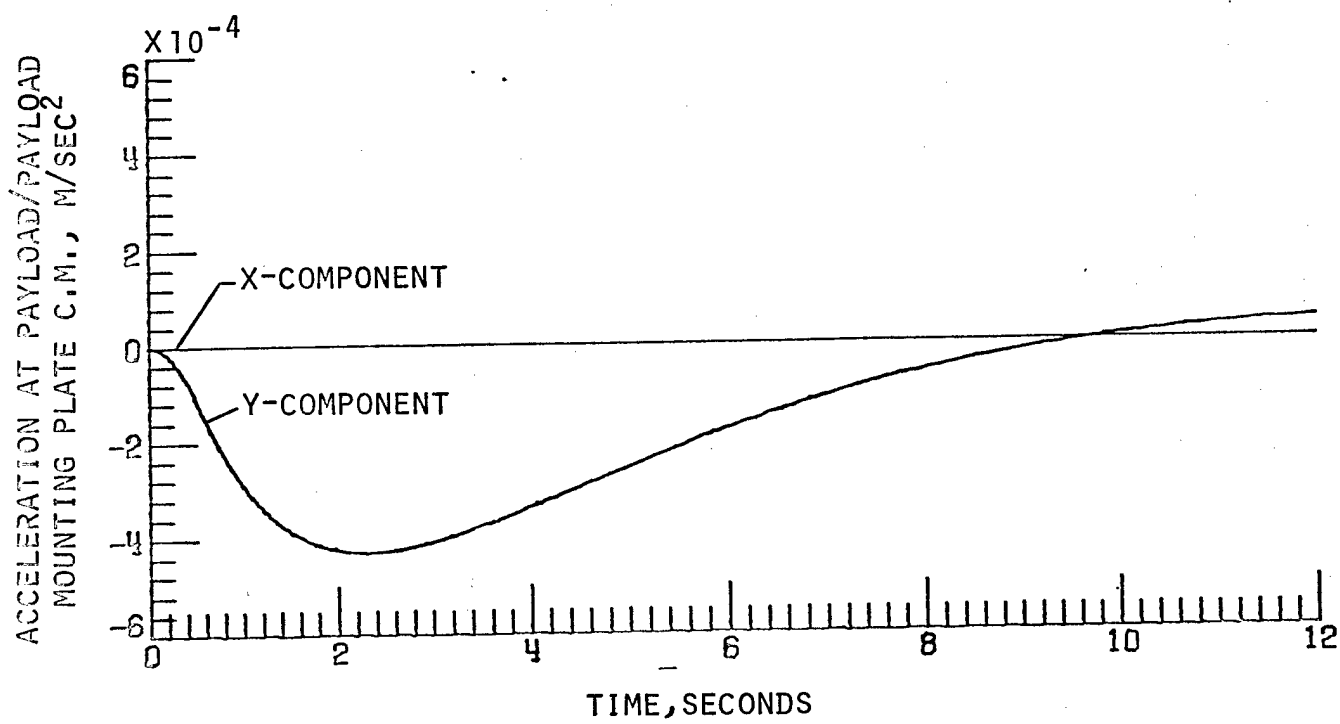
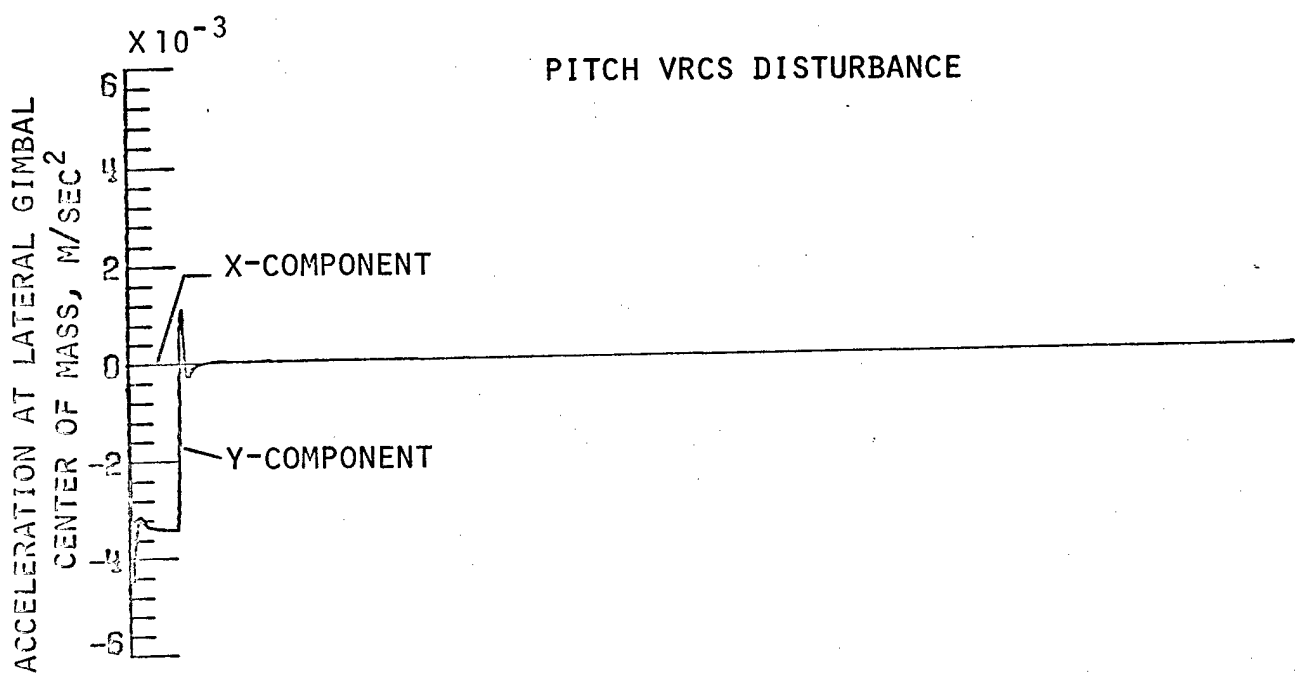


Figure 19(a).- Time history of acceleration perpendicular to LOS (in $X_p - Y_p$ plane) measured at the lateral gimbal and at the payload/payload mounting plate center of mass (Initial conditions $\sigma = -86^\circ$, $\gamma = 0^\circ$).

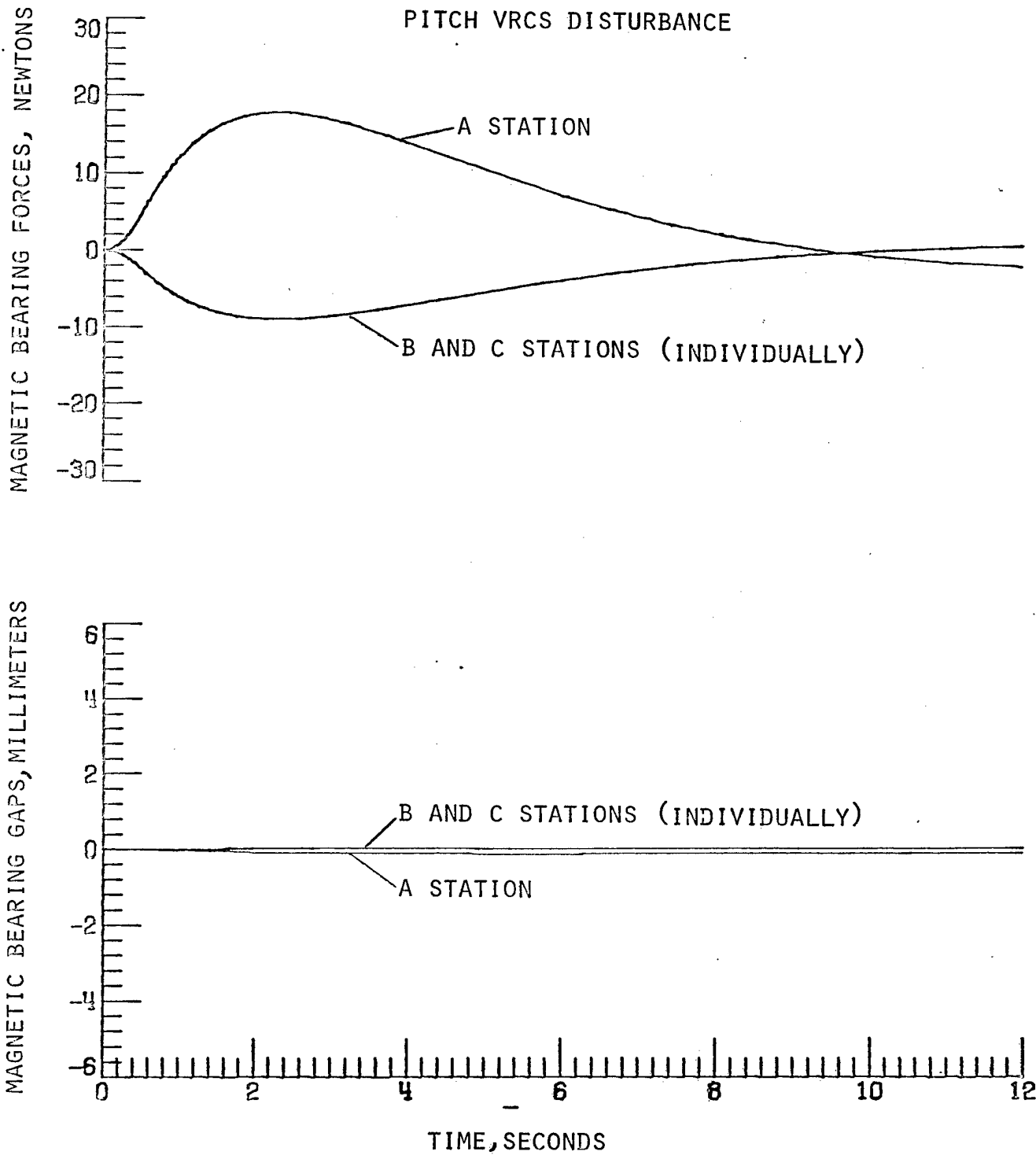


Figure 19(b).- Time histories of axial MBA forces and gaps
(Initial conditions $\sigma = -86^\circ$, $\gamma = 0^\circ$).

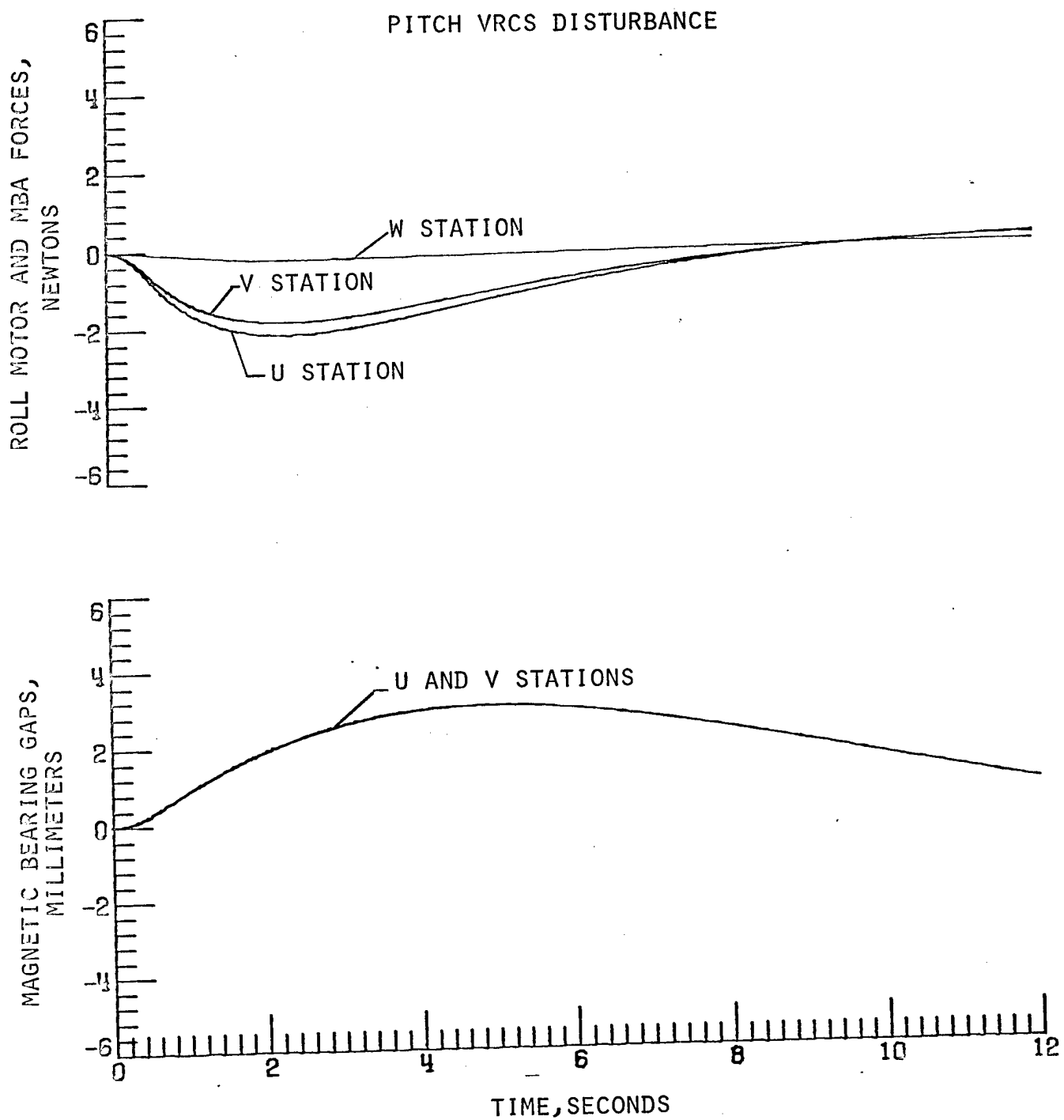
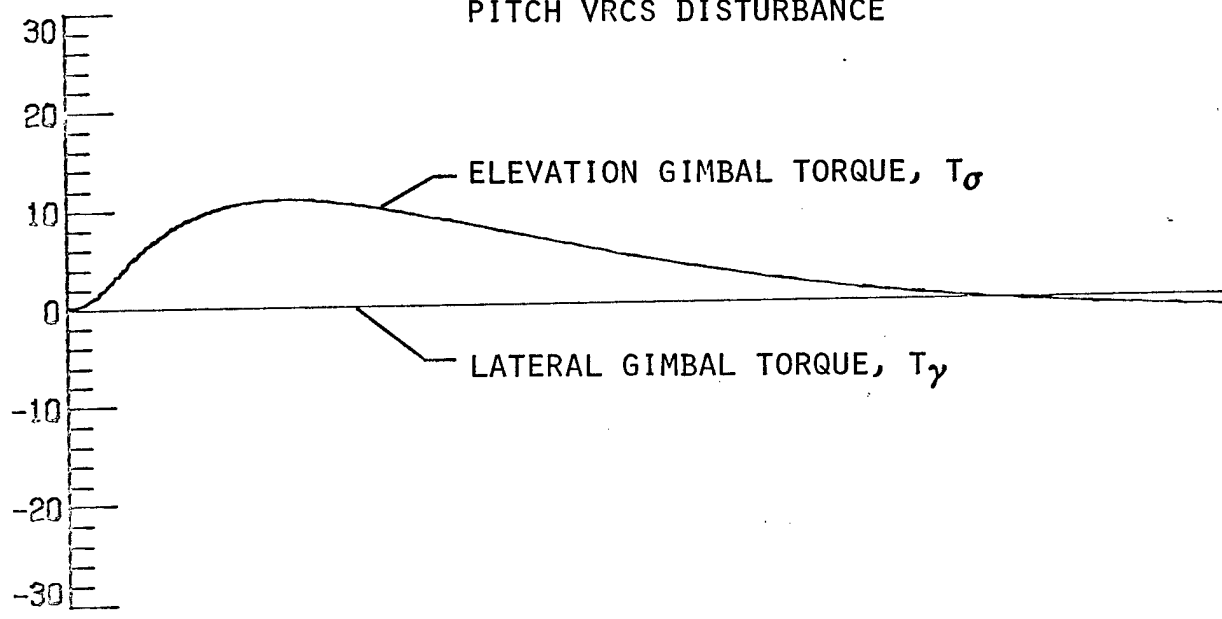


Figure 19(c).- Time histories of radial MBA and roll motor forces and MBA gaps (Initial conditions $\sigma = -86^\circ$, $\gamma = 0^\circ$).

GIMBAL TORQUES, N-M

PITCH VRCS DISTURBANCE



POINTING ERROR, ARCSECONDS

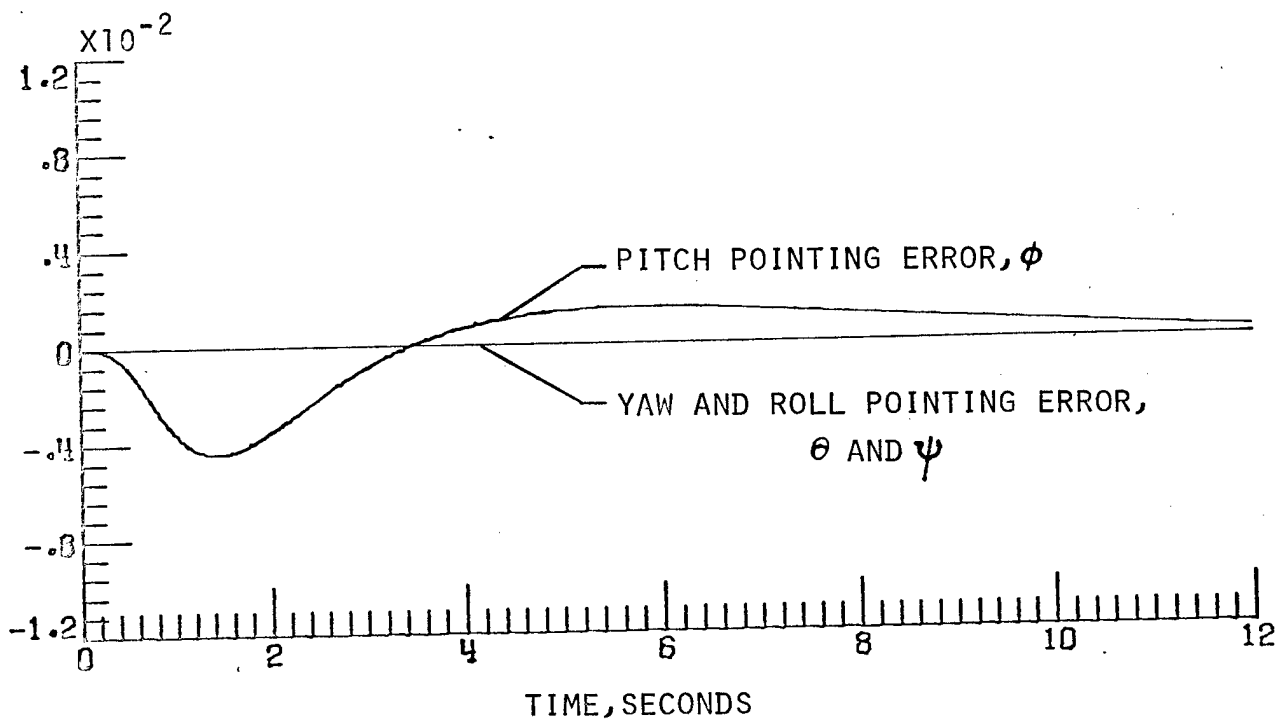


Figure 19(d).- Time histories of gimbal torques and payload pointing errors. (Initial conditions $\sigma = -86^\circ$, $\gamma = 0^\circ$)

TABLE 1

SOT CHARACTERISTICS AND REQUIREMENTS

4	Mass	6600 kg
5	Size	3.8 meters diameter 7.3 meters length
6	Inertia (referenced through c.m.)	
7	I _x	3.8 x 10 ⁴ kg-m ²
8	I _y	1.6 x 10 ⁴ kg-m ²
9	I _z	4.4 x 10 ⁴ kg-m ²
10	Center of Mass (from base of payload)	
11	X _{SOT}	0.03 meters
12	Y _{SOT}	3.44 meters
13	Z _{SOT}	0.37 meters
14	Pointing Accuracy	± 0.5 arcsec LOS ± 60 arcsec roll
15	Pointing Stability	0.08 arcsec LOS 10 arcsec roll
16	Stability Rate	5 arcsec/sec
17	Pointing Acquisition	± 1 arcsec
18	Field of View	± 180 arcsec
19	Maximum Jitter	≤ 5 arcsec/sec
20	Pointing Duration	60 minutes
	Long Term Stability Duration	900 seconds
	Short Term Stability Duration	10 seconds

TABLE 2.- ASPS RESPONSE TO CREW MOTION AND VRCS DISTURBANCE

Disturbance	Initial Gim. Angles (deg)		Max A ₁ LOS (Meters/sec ²)		Max. MBA Force (Newtons)				Max. Gim. Torque (Newton-Meters)		Max. Ptg. Error (Arcseconds)			
	σ	γ	At Lat. Gim	At P/L	A	B	C	U	V	T_σ	T_γ	ϕ	θ	ψ
Crew Motion	-86	0	0.00086	0.000069	2	-2.8	0.9	0.3	-0.7	1.2	-1.2	-0.0006	-0.0015	0
+ Pitch VRCS with Crew Motion	-86	0	0.00447	0.000477	19.8	-12	-8	-2	-2.6	12	-1.2	-0.005	0.005	0
- Pitch VRCS	78	0	0.0017	0.00016	-6.6	3.3	3.3	8.0	6.8	-4.1	0	0.0017	0	0
Crew Motion	78	0	0.0011	0.000079	-2.2	-1.0	3.2	0.82	-0.33	-1.34	-1.4	-0.0007	-0.0018	0
- Pitch VRCS with Crew Motion	78	0	0.0018	0.00022	-8.7	2.3	6.5	1.6	0.49	-5.4	-1.4	0.0022	-0.0018	0
Crew Motion	0	-40	0.000956	0.0000756	-0.46	2.9	-2.4	-0.64	0.75	-0.11	1.8	-0.00014	0.0023	0
+ Roll VRCS with Crew Motion	0	-40	0.0044	0.00026	-0.46	9.4	-9	-2.3	2.5	2.0	6.2	-0.00014	-0.0062	0.00024
+ Pitch VRCS with Roll VRCS	-86	-40	0.0043	0.00055	22	-7.5	-15	-3.7	-1.4	10.9	2.6	-0.0054	-0.0026	0.00028

Values for + Pitch VRCS and + Roll VRCS are available from figures 7 through 18

1. Report No. TM-80136	2. Government Accession No.	3. Recipient's Catalog No.	
4. Title and Subtitle Determination of ASPS Performance for Large Payloads in the Shuttle Orbiter Disturbance Environment		5. Report Date October 1979	
		6. Performing Organization Code	
7. Author(s) Claude R. Keckler, Kemper S. Kibler, and Lawrence F. Rowell		8. Performing Organization Report No.	
9. Performing Organization Name and Address NASA Langley Research Center Hampton, Virginia 23665		10. Work Unit No. 506-61-73-04	
		11. Contract or Grant No.	
		13. Type of Report and Period Covered Technical Memorandum	
12. Sponsoring Agency Name and Address National Aeronautics and Space Administration Washington, DC 20546		14. Army Project No.	
15. Supplementary Notes			
16. Abstract Projected mission models for the next decade include large facility class payloads which demand high accuracy pointing and stability capabilities far in excess of the space Shuttle. To accommodate these requirements, proposals have been made which include the use of advanced, sophisticated payload pointers, or conventional gimbal arrangements in conjunction with extensive, payload unique, image motion compensation systems. A candidate advanced payload pointer is the Annular Suspension and Pointing System (ASPS). Since this device is intended to satisfy a large variety of payload requirements and mission objectives, it is necessary to establish its performance in the expected operational environment. Using a high fidelity, multi-degree of freedom, digital simulation, an evaluation of the ASPS capability in satisfying facility class payload requirements, while being subjected to the Shuttle disturbance environment, was performed.			
17. Key Words (Suggested by Author(s)) Payload pointer, ASPS, facility class payload, disturbance environment, high accuracy pointing and stability	18. Distribution Statement Unclassified - Unlimited		
STAR Categories 18 31 37 66			
19. Security Classif. (of this report) Unclassified	20. Security Classif. (of this page) Unclassified	21. No. of Pages 35	22. Price* \$4.50